Science of the Total Environment 572 (2016) 755–769

Contents lists available at ScienceDirect

Science of the Total Environment

journal homepage: www.elsevier.com/locate/scitotenv

Ground-level air pollution changes during a boreal wildland mega-fire☆

Andrzej Bytnerowicz [a,*], Yu-Mei Hsu [b], Kevin Percy [b], Allan Legge [c], Mark E. Fenn [a], Susan Schilling [a], Witold Frączek [d], Diane Alexander [a]

[a] USDA Forest Service, Pacific Southwest Research Station, 4955 Canyon Crest Drive, Riverside, CA 92507, USA
[b] Wood Buffalo Environmental Association, #100-330 Thickwood Blvd., Fort McMurray, Alberta, T9K 1Y1, Canada
[c] Biosphere Solutions, Calgary, Alberta, T2N 1H7, Canada
[d] Environmental Systems Research Institute, Redlands, CA 92373, USA

HIGHLIGHTS

- Boreal mega-fire increased $PM_{2.5}$, NH_3, HONO, HNO_3, NH_4^+ and NO_3^- at receptor site.
- Elevated ambient NH_3 and HNO_3 lasted several months across northern Alberta.
- Higher NH_3 and HNO_3 contributed to increased N deposition to boreal forests.

GRAPHICAL ABSTRACT

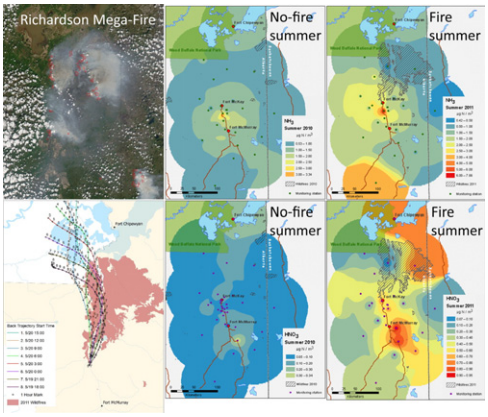

ARTICLE INFO

Article history:
Received 17 May 2016
Received in revised form 6 July 2016
Accepted 7 July 2016
Available online 13 September 2016

Editor: Elena Paoletti

Keywords:
Fine particulate matter
Reactive nitrogenous species
Sulfur dioxide
Sulfate
Ozone

ABSTRACT

The 2011 Richardson wildland mega-fire in the Athabasca Oil Sands Region (AOSR) in northern Alberta, Canada had large effects on air quality. At a receptor site in the center of the AOSR ambient $PM_{2.5}$, O_3, NO, NO_2, SO_2, NH_3, HONO, HNO_3, NH_4^+ and NO_3^- were measured during the April–August 2011 period. Concentrations of NH_3, HNO_3, NO_2, SO_2 and O_3 were also monitored across the AOSR with passive samplers, providing monthly summer and bi-monthly winter average values in 2010, 2011 and 2012. During the fire, hourly $PM_{2.5}$ concentrations >450 μg m^{-3} were measured at the AMS 1 receptor site. The 24-h National Ambient Air Quality Standard (NAAQS) of 35 μg m^{-3} and the Canada Wide Standard (CWS) of 30 μg m^{-3} were exceeded on 13 days in May and 7 days in June. During the fire emission periods, sharp increases in NH_3, HONO, HNO_3, NH_4^+, NO_3^- and total inorganic reactive N concentrations occurred, all closely correlated with the $PM_{2.5}$ changes. There were large differences in the relative contribution of various N compounds to total inorganic N between the no-fire emission and fire emission periods. While in the absence of fires NO and NO_2 dominated, their relative contribution during the fires was ~2 fold smaller, mainly due to increased NH_3, NH_4^+ and NO_3^-. Concentrations of HONO and HNO_3 also greatly increased during the fires, but their contribution to the total inorganic N pool was relatively small. Elevated NH_3 and HNO_3 concentrations affected large areas of northern Alberta during the Richardson Fire. While NH_3 and HNO_3 concentrations were not at levels considered toxic to plants, these gases contributed

☆ Capsule: Boreal mega-fire caused a sharp increase in ambient $PM_{2.5}$, NH_3, HONO, HNO_3, NH_4^+ and NO_3^- near the fires as well as long-lasting and widespread occurrence of elevated NH_3 and HNO_3.

* Corresponding author.
E-mail addresses: abytnerowicz@fs.fed.us (A. Bytnerowicz), mfenn@fs.fed.us (M.E. Fenn).

http://dx.doi.org/10.1016/j.scitotenv.2016.07.052
0048-9697/Published by Elsevier B.V.

significantly to atmospheric N deposition. Generally, no significant changes in O_3 and SO_2 concentrations were detected and their ambient concentrations were below levels harmful to human health or sensitive vegetation.
Published by Elsevier B.V.

1. Introduction

Large wildland fires burning over 10,000 ha are termed mega-fires. Such fires cause severe degradation of air quality, impacting human health and ecological processes to varying degrees (Stephens et al., 2014). Mega-fires are also major sources of greenhouse gases with severe consequences for climate change (Liu et al., 2014). The Richardson Fire was the second largest wildland mega-fire in the history of Alberta, Canada. It was located north of the city of Fort McKay in an area known as the Richardson Backcountry. The fire started on May 15th, 2011 and reached 16,000 ha overnight (Gregory, 2012). The fire rapidly spread through the Athabasca Oil Sands Region (AOSR) until the end of June (Fig. 1) when its progression slowed as rain and cooler weather prevailed in the region. Large areas of boreal forest, especially on the eastern flanks of the AOSR, were allowed to burn into August due to the absence of human settlements or oil facilities in those areas. By the end of summer 2011 when the fire was fully contained, over 700,000 ha of forest burned (https://en.wikipedia.org/wiki/Richardson_fire).

Wildland fires produce large amounts of smoke which is defined as an aerosol consisting mainly of water vapor, primary gases, volatile organic compounds (VOCs), semi-volatile organic compounds (SVOCs) and particles (Andreae and Merlet, 2001). Primary gases released from fires include carbon monoxide (CO), carbon dioxide (CO_2) as well as nitrogen oxides (NO_x), ammonia (NH_3) and sulfur dioxide (SO_2) (Conard and Ivanova, 1998; Goldammer et al., 2009). Secondary gases, produced during reactions of the primary gases, include ozone (O_3) formed by complex photochemical reactions of VOCs and NO_x (Urbanski et al., 2009), and nitric acid (HNO_3) generated by reactions between nitric oxide (NO), nitrogen dioxide (NO_2), as well as the oxygen and hydroxyl radicals (O and OH, respectively) (Seinfeld and Pandis, 2006). Particles in wildland fire smoke are predominantly in the fine mode (diameter ≤ 2.5 μm) (http://www3.epa.gov/airtrends/aqtrnd04/pmreport03/pmunderstand_2405.pdf; Saarnio et al., 2010) and mainly consist of elemental carbon (soot), organic carbon and various organic compounds (Goldammer et al., 2009). The less-prominent inorganic fraction of fine smoke particles includes ammonium (NH_4^+), nitrate (NO_3^-) and sulfate (SO_4^{2-}) ions forming semi-volatile compounds such as NH_4NO_3 and $(NH_4)_2SO_4$ (Schaap et al., 2004). These compounds result from complex reactions of NO_x, sulfur oxides (SO_x), nitrous acid (HONO), HNO_3 and NH_3 in smoke plumes (Akagi et al., 2012). The inorganic fraction of smoke particulate matter also contains water-soluble ions such as potassium, sodium, magnesium, calcium, and chloride as well as various trace elements (Goldammer et al., 2009; Hays et al., 2002). Carbon monoxide, CO_2, VOCs, SVOCs, elemental carbon and NO_x emitted from wildland fires contribute significantly to changing global temperatures either directly or indirectly by producing such compounds as O_3 (a greenhouse gas) or particulate NO_3^-, the latter causing negative radiative forcing (IPCC, 2013).

Various air pollutants released directly from wildland fires, and those formed during secondary reactions in smoke plumes, negatively affect human health. These toxic compounds include NO_x, SO_x, O_3 and numerous organic gases and aerosols, many of them carcinogenic (Fowler, 2003; Goldammer et al., 2009). Biomass burning that leads to elevated levels of $PM_{2.5}$ is associated with serious human health problems (Kinney, 2008; Koelemeijer et al., 2006). Significant impacts on ecosystem health can be caused by elevated concentrations of O_3, NO_2, SO_2 and HNO_3 well-known for their phytotoxic effects on sensitive vegetation (Bytnerowicz et al., 2007). Nitrogen oxides, NH_3, HONO, HNO_3, as well as particulate NH_4^+ and NO_3^- are important components of reactive atmospheric nitrogen and major drivers of atmospheric dry deposition of nitrogen (N) to forests and other ecosystems (Hanson and Lindberg, 1991; Lovett, 1994; Pinder et al., 2012). Knowledge of ambient concentrations of N air pollutants is important for understanding their potential phytotoxic effects on sensitive vegetation and for estimates of N dry deposition to forests and other ecosystems. Ambient air quality of the AOSR has been monitored from a perspective of potential impacts of emissions from oil exploration and processing on the boreal forest and wetland ecosystems (Percy, 2013; Percy et al., 2012). For that purpose, a passive sampler monitoring network for ecologically important air pollutants such as NO_2, HNO_3, NH_3, SO_2 and O_3 has been developed (Bytnerowicz et al., 2010b; Fenn et al., 2015; Hsu and Bytnerowicz, 2015; Hsu and Clair, 2015). No indications of direct

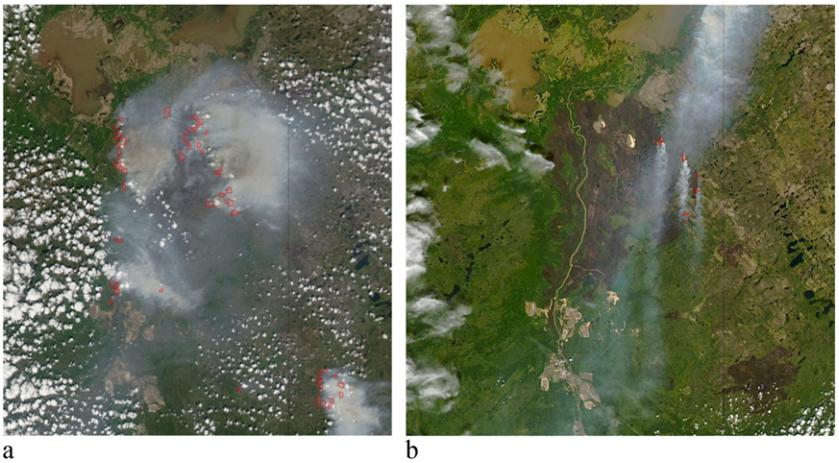

Fig. 1. Progression of the Richardson Fire shown as images obtained on June 8, 2011 (a) and June 26 (b) from the Moderate Resolution Imaging Spectroradiometer (MODIS), the Aqua satellite. Under thick smoke a cluster of wildfires are outlined in red. Dark brown burn scars seen on the June 26th image define the areas burned by the Richardson Fire (center of the AOSR), and in Saskatchewan (SE section of the image).

phytotoxic effects of these pollutants have been found, although elevated N and S deposition in the vicinity of the industrial center of the AOSR has been reported (Fenn et al., 2015; Hsu and Bytnerowicz, 2015).

Improved understanding of the potential impacts of large wildland fires on ambient air quality is important for evaluating environmental risks to human and ecosystem health. Knowledge of the impacts of wildland fire emissions on the ambient air chemistry of N compounds is particularly limited, although elevated concentrations of NH_3, HONO and HNO_3 have been reported from areas affected by wildland fires (Andreae and Merlet, 2001; Burling et al., 2011; Bytnerowicz et al., 2000; Hegg et al., 1988; LeBel et al., 1988). Information presented in this article attempts to fill this knowledge gap, especially from a perspective of changes in inorganic N air pollutants. This has been done by comparing the "fire emission" and "no-fire emission" periods over timescales of months, seasons and years. Changes in ambient concentrations of inorganic N and S compounds, $PM_{2.5}$ and O_3 were investigated at a receptor site directly affected by emissions from the Richardson wildland mega-fire. This was done by intensive real-time monitoring of nitrogenous and sulfurous gaseous and aerosol pollutants, as well as O_3 and $PM_{2.5}$ at a location in the center of the AOSR and adjacent to the area impacted by the Richardson Fire. Information on spatial and temporal changes of NO_2, HNO_3, NH_3, SO_2 and O_3 concentrations for the entire AOSR area was obtained from the passive sampler monitoring network described above.

2. Methods

2.1. Monitoring activities

Real-time air quality monitoring was performed at the Bertha Ganter-Fort McKay (AMS 1) monitoring station located in the center of AOSR (−111.64045°W; 57.18945°N). The AMS 1 station was near the southern edge of the 2011 Richardson Fire. $PM_{2.5}$, O_3, NO and NO_2 were monitored with the US EPA Federal Equivalent Methods (FEMs) and Federal Reference Methods (FRMs). Concentrations of inorganic gaseous phase species, including NH_3, HONO, HNO_3, and SO_2, as well as particulate phase species, including NH_4^+, NO_3^-, and SO_4^{2-} were monitored with the ambient ion monitoring - ion chromatography (AIM-IC) system. Monitoring of ambient NH_3, HNO_3, NO_2, SO_2 and O_3 near the mining and industrial operations and in remote forest health evaluation sites was performed with passive samplers providing monthly average concentrations in summer (April through September) and bi-monthly concentrations in winter (October through March). Passive samplers were exposed to ambient air above the forest canopy (on towers) or on 2 m high posts in the industrial areas and wetlands. During the 2010–2012 monitoring campaigns all pollutants were monitored at 27 sites. In 2010, NH_3 and HNO_3 were monitored on a denser network with 13 additional sites (Fig. 2).

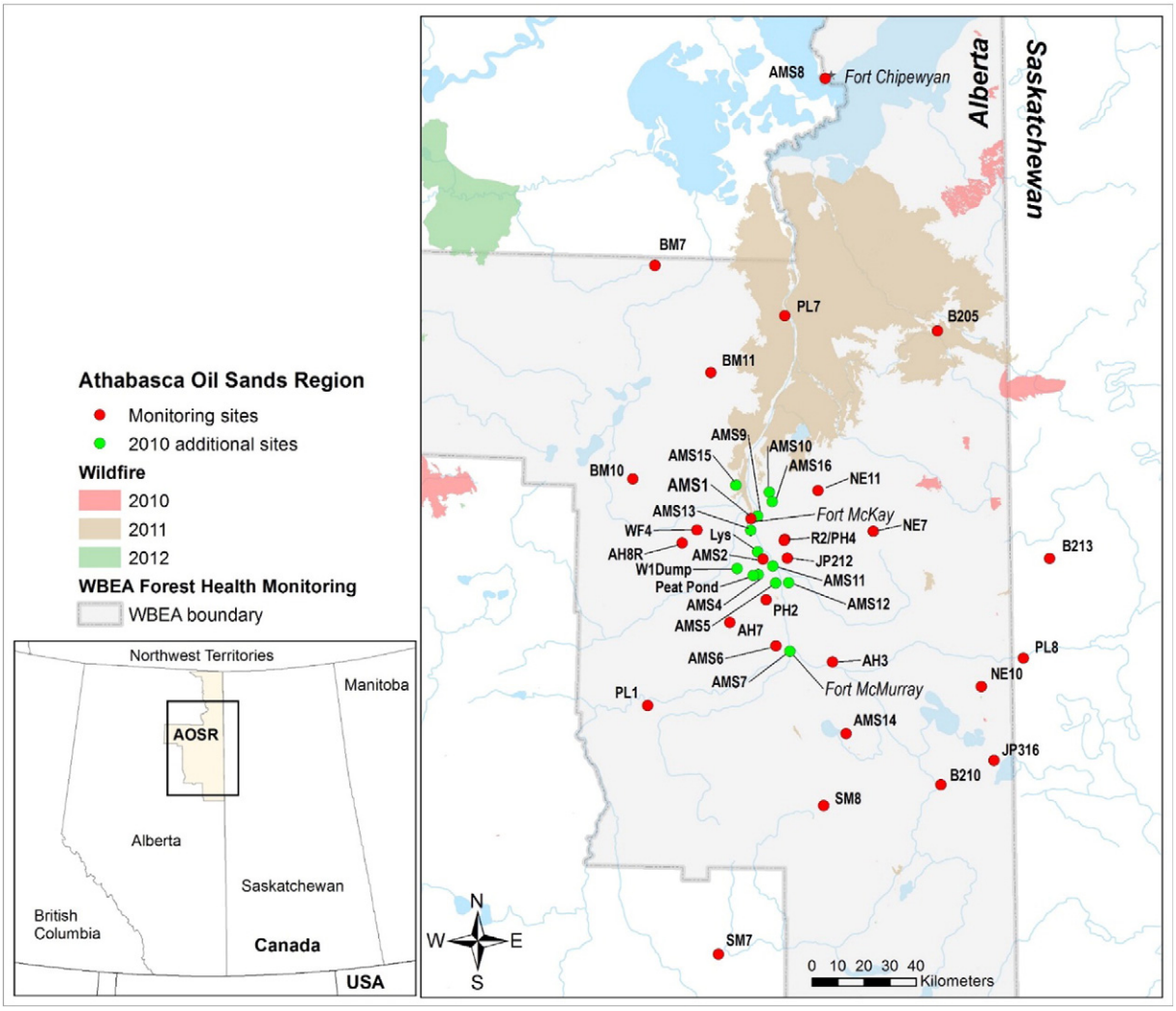

Fig. 2. The passive sampler air quality monitoring network established and coordinated by the Wood Buffalo Environmental Association (WBEA) and perimeters of wildland fires in 2010, 2011 and 2012 in the Athabasca Oil Sands Region (AOSR). The network consisted of 27 monitoring sites for NH_3, HNO_3, NO_2, SO_2 and O_3. In 2010 there were additional 13 sites for NH_3 and HNO_3 monitoring.

2.2. $PM_{2.5}$, O_3, and NO/NO_2 real-time monitoring

Hourly $PM_{2.5}$, O_3, NO and NO_2 concentrations were monitored by FEMs and FRMs. The real time monitors included a Tapered Element Oscillating Microbalance (TEOM) monitor (Model 1400a, Thermo Scientific) (with a maximum detection set at 450 μg m^{-3}) before May 31, 2011 and a Synchronized Hybrid Ambient Real-time Particulate (SHARP) monitor (Model 5030, Thermo Scientific) after May 31, 2011 for $PM_{2.5}$; an O_3 analyzer (Model 49C, Thermo Electron); and an NO_x analyzer (Thermo Environmentals Model 42C) for NO and NO_2. Routine maintenance for the SHARP monitor was conducted monthly. For both O_3 and NO_x analyzers, daily zero span and monthly calibration were conducted. The standard operation procedures are listed in http://wbea.org/air-monitoring/standard-operating-procedures.

2.3. NH_3, HONO, HNO_3, SO_2, NH_4^+, NO_3^-, and SO_4^{2-} real-time monitoring

The AIM-IC system consisted of the ambient ion monitor (model AIM 9000D) for collection of inorganic gases (NH_3, HONO, HNO_3, and SO_2), and two ion chromatography (IC) systems (model ICS-2000) for the analyses of anions and cations (NH_4^+, NO_3^-, and SO_4^{2-}). After ambient air entered the AIM-IC system, gases phase species were collected by a parallel-plate wet denuder and the water soluble inorganic particulate species by a particle super saturation chamber with a collection cyclone. After 1 h of sampling, the samples were injected onto two IC systems for simultaneous anion and cation analyses (Hsu and Clair, 2015).

2.4. NH_3, HNO_3, NO_2, SO_2 and O_3 passive sampler monitoring

Passive samplers with two replicate cellulose filters coated with citric acid of the Ogawa design (Roadman et al., 2003) were used for NH_3 monitoring. Ammonia reacts with citric acid producing ammonium citrate. After water extraction, ammonium (NH_4^+) concentrations in filter extracts were determined colorimetrically on a TRAACS 2000 Autoanalyzer, and ambient NH_3 concentrations were calculated based on a comparison of passive samplers against the collocated honeycomb denuder systems (Koutrakis et al., 1993). Three replicate HNO_3 samplers (Bytnerowicz et al., 2005) were used at each monitoring site. In these samplers, ambient air passes through a Teflon membrane and gaseous HNO_3 and HONO are absorbed on a Nylasorb nylon filter as nitrate (NO_3^-). Nylon filters from the samplers were extracted in nano-pure water, and NO_3^- concentrations in filter extracts were analyzed by ion chromatography (Dionex ICS 2000 LCD). The results for this study were calculated using calibration curves developed by comparing the passive samplers against the collocated honeycomb denuder systems (Bytnerowicz et al., 2005; Koutrakis et al., 1993). Our results are expressed as HNO_3 concentrations with an understanding that HONO contributes to these results (Bytnerowicz et al., 2005). Exposed HNO_3 and NH_3 samplers were shipped to the USDA FS chemical laboratory in Riverside, California, where filters from the samplers were extracted. Precision of NH_3 and HNO_3 passive samplers was 12% and 13%, respectively. An all-season NO_2 passive sampling system (NPSS) (Tang et al., 1999), a SO_2 passive sampling system (SPSS) (Tang et al., 1997), and an O_3 passive sampling system (OPSS) (Tang and Lau, 2000) were used to determine concentrations of NO_2, SO_2 and O_3, respectively. The collection media were CHEMIX™ for NO_2, a sodium carbonate coated filter for SO_2 and a sodium nitrite coated filter for O_3. After field exposure, NO_2, SO_2, and O_3 filter samples were extracted with distilled/deionized water and analyzed by ion chromatography (DX-120, Dionex Corp., US) for NO_2^-, SO_4^{2-}, and NO_3^- concentrations, respectively, by Maxxam Analytic Inc. Depending on the location, duplicate or triplicate samplers were applied for data validation. The ambient concentration was calculated as total mass of analyzed species on the filter divided by the total air volume passing through the filter. Sampling flow rates of SO_2, NO_2 and O_3 passive samplers were calculated by developed equations with known temperature, relative humidity and wind speed at each site. Precision of NO_2, SO_2 and O_3 passive samplers were 13%, 16% and 5%, respectively (Hsu, 2013).

2.5. Meteorological determinations

Meteorological monitoring was conducted at the AMS 1 site. A Campbell Scientific probe HMP35C212 was used for collection of temperature and relative humidity (RH) data. Met One Instruments sensors 010C and 020C were used for monitoring wind speed and wind direction, respectively. All meteorological data and detailed information on monitoring methodologies are available at: www.wbea.org. Frequency of wind direction counts was presented as a wind-rose in which each wind direction spoke showed apportionment of $PM_{2.5}$ concentrations in seven ranges: 0–5; 5–15; 15–25; 25–35; 35–50; 50–100; and 100–500 μg m^{-3}.

2.6. Backward trajectories

The Air Resource Laboratory (ARL) HYSPLIT Trajectory Model (http://www.ready.noaa.gov/HYSPLIT.php) was used to compute archived trajectories for tracking movement of air masses into the receptor site (AMS1). Meteorology data used was from the EDAS40 (Eta Data Assimilation System). The vertical motion method used was "Model Vertical Velocity". Start time of the first trajectory was set as UTC 5/20/2011 22:00 (MST 5/20/11 15:00) at 30 m above ground level with a 24 h running time. Additional back-trajectories were requested at 3-h intervals going back to MST 5/19/2011 18:00. GIS data generated by the model was mapped using ESRI ArcGIS software.

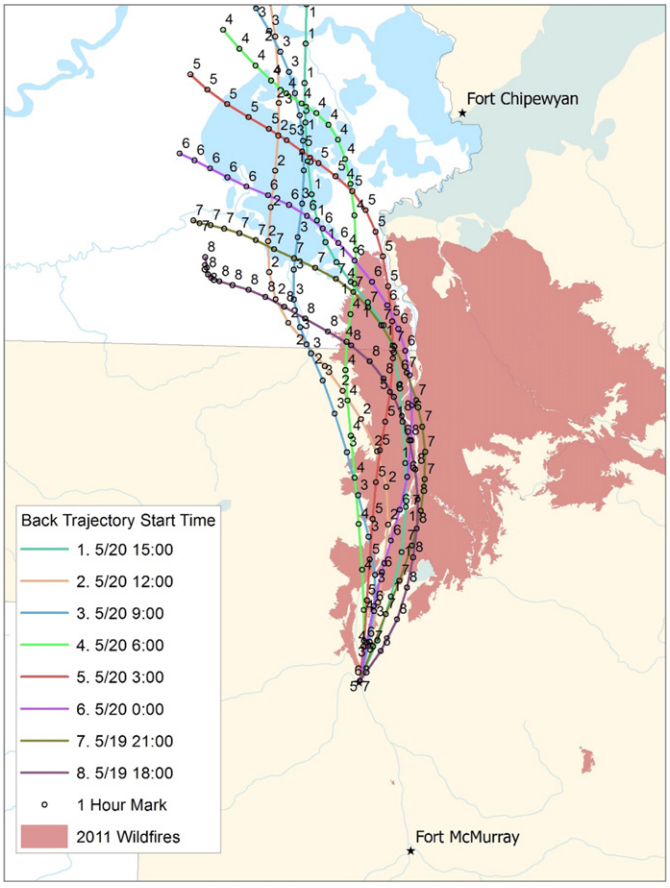

Fig. 3. 24-h backward trajectories at the AMS 1 receptor site at Fort McKay during the high pollution days of May 19 and 20, 2011. Markers on each line represent hourly positions. The backward trajectories were calculated starting from eight different times shown in the legend.

2.7. Geostatistical maps

Air pollutant distribution maps based on the NH_3 and HNO_3 passive sampler results were developed with inverse distance weighted (IDW) methods using Geostatistical Analyst, an extension of the ESRI ArcGIS software. This method was selected because for the given data, characterized by a relatively low number of monitoring sites, high spatial variation, and lack of trends or spatial patterns, it provided the most accurate results (Johnston et al., 2001). Concentration distribution maps of NH_3 and HNO_3 were made for summer 2010, 2011 and 2012 and for individual months (April through September) in 2011. Data from 40 sites were used for the 2010 maps and from 27 sites for the 2011 and 2012 maps. Concentrations of NH_3 and HNO_3 in geostatistical maps are expressed in μg N-NH_3 m^{-3} and μg N-HNO_3 m^{-3}.

2.8. Statistical analysis of data

Significance of the effects of fire emissions on concentrations of measured chemical species was calculated with a one-way unbalanced ANOVA (GLM) using the Tukey means comparison at $P = 0.05$. For these calculations the SAS/STAT® software was used (copyright: SAS Institute Inc. SAS and all other SAS Institute Inc. product or service names are registered trademarks or trademarks of SAS Institute Inc., Cary, NC, USA). Sigma Plot 11.0 was used for generating graphs, and box plots were based on the Rank Sum Test. The wind-rose/$PM_{2.5}$ graph was developed using the "openair" package running in *R*3.2.2 (R Core Team, 2015; Carslaw and Ropkins, 2016).

3. Results

3.1. AMS 1 site in the center of the AOSR monitoring network

3.1.1. Particulate matter

The Richardson Fire started on May 15, 2011 and immediately influenced the air pollution status of the AMS 1 receptor site. Backward trajectories for May 20, 2011 provide an example of high-pollution days when air masses reached that site after sweeping over the fire-affected areas (Fig. 3). In the absence of fire emissions (April, July and most of August), $PM_{2.5}$ concentrations were low and stayed below 25 μg m^{-3} (Figs. 4, 5). Consequently, periods when $PM_{2.5}$ concentrations were <25 μg m^{-3} were designated as "no-fire emission", while those with $PM_{2.5}$ values ≥25 μg m^{-3} as the "fire emission" periods. Our designation of "no-fire emission" vs. "fire-emission" periods with the $PM_{2.5}$ cut-off point of 25 μg m^{-3} was the same as in the analyses of fire emissions in boreal forests of Europe (Saarnio et al., 2010). The $PM_{2.5}$ concentrations abruptly increased at the outbreak of the Richardson Fire on May 15th reaching or exceeding hourly maxima of 450 μg m^{-3} (maximum detection set for the instrument) during most days until the end of May. The maximum 24 h average concentration during this period was 368.0 μg m^{-3} (Fig. 5a, b). In May the daytime and nighttime $PM_{2.5}$ averages were 175.7 μg m^{-3} and 187.4 μg m^{-3},

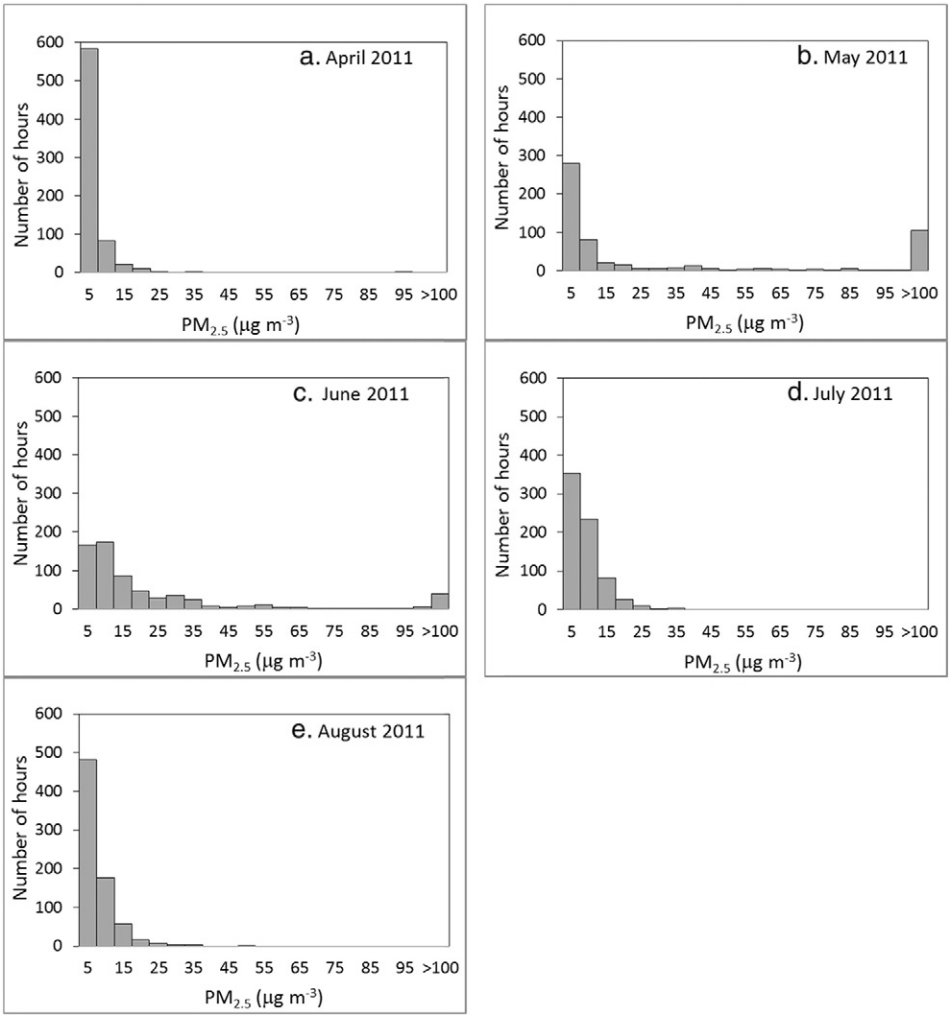

Fig. 4. Histograms of $PM_{2.5}$ frequency distribution at the AMS 1 monitoring station before, during and after emission impacts of the 2011 Richardson Fire; (a) April (before); (b) May (during); (c) June (during): (d) July (after); and (e) August (after).

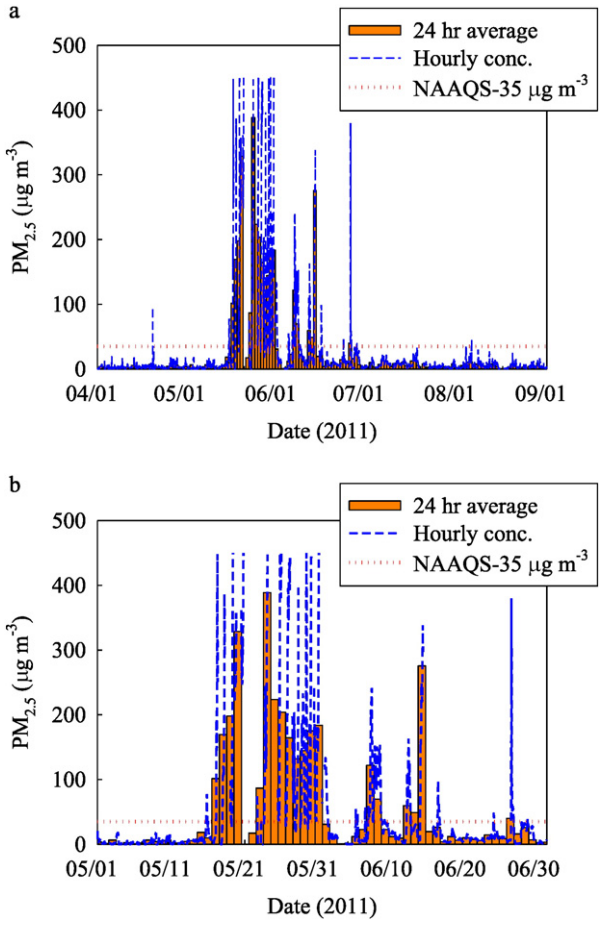

Fig. 5. Concentrations of fine particulate matter ($PM_{2.5}$) at the AMS 1 monitoring site during the Richardson Fire of summer 2011; a. entire monitoring period of April 1–September 1, 2011; b. detailed high-pollution period of May 1–June 30, 2011. Note that the upper limit of the $PM_{2.5}$ monitoring instrument was set at 450 μg m^{-3}.

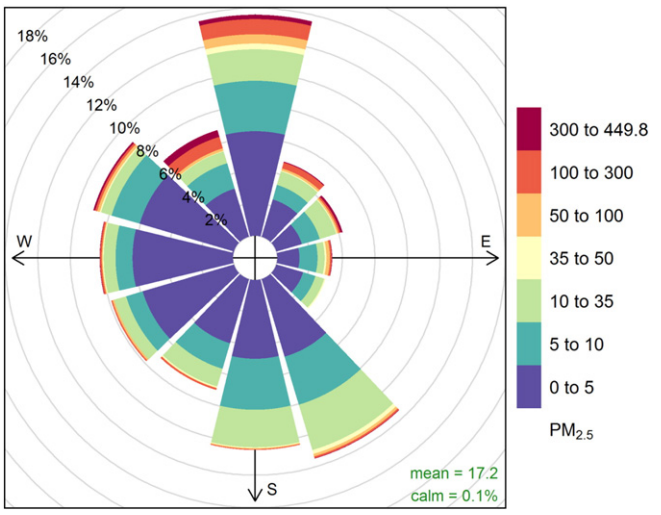

Fig. 6. Wind rose for $PM_{2.5}$ of different concentration ranges (μg m^{-3}) during the entire monitoring period of April 1–September 1, 2011. Values in the lower right-hand side of the graph: mean of 17.2 refers to the mean $PM_{2.5}$ concentration during the monitoring period; calm refers to percent of time when wind speed was below the measurement threshold of 0.1%.

respectively (Table 1). In June, maximum hourly concentrations exceeded 300 μg m^{-3} only on a few occasions, while the highest 24 h average was 271.1 μg m^{-3} (Fig. 5). In June the daytime and nighttime average $PM_{2.5}$ concentrations were much lower than in May - 60.9 and 98.7 μg m^{-3}, respectively (Table 1). The U.S. National Ambient Air Quality Standard (NAAQS) for $PM_{2.5}$ of 35 μg m^{-3} and the Canada Wide Standard (CWS) of 30 μg m^{-3} (24-h average) were exceeded on 20 days (13 in May and 7 in June) during the Richardson Fire. The highest $PM_{2.5}$ values occurred with winds coming from the NW and N directions (Fig. 6).

3.1.2. Nitrogenous species

Concentrations of NH_3 increased during the fire emission periods compared with the no-fire emission periods. Similar increases were noted for the daytime and nighttime periods. Concentrations of NH_3 were higher in May (~7 fold greater than no-fire periods) than in June (~2 fold greater than no-fire periods). Concentrations of NO did not change during the fire emission periods during daytime, however they increased at nighttime (1.5 fold in May and 1.6 in June). Daytime concentrations of NO_2 increased during the fire emission periods by 1.6 fold in May and 1.7 fold in June. Nighttime NO_2 concentrations increased 2.3 fold in May and 1.3 in June. Concentrations of HONO increased by 8.0 fold in May and 3.0 fold in June in daytime, and by 13.0 fold in May and 3.7 fold in June at nighttime. Nitric acid concentrations were elevated in daytime by 7.5 fold in May and 2.0 fold in June, and at nighttime by 7.3 fold in May and 2.5 fold in June. The $N\text{-}HNO_3$/N-HONO ratios were higher in daytime than at nighttime. For the fire emission periods these ratios were 1.88 in May and 2.00 in June, and for the no-fire emission periods 2.00 in May and 3.00 in June. The nighttime ratios were lower during the fire periods (0.85 in May and 0.91 in June) compared with the no-fire periods (1.50 in May and 1.33 in June). There was a large increase in NH_4^+ concentrations during fire emission periods. In daytime these increases were 3.9 fold in May and 2.7 fold in June, while those for the nighttime were 5.6 fold in May and 3.0 fold in June. The increase in NO_3^- concentrations during the fire periods was

Table 1
Average concentrations of nitrogenous air pollutants and fine particulate matter ($PM_{2.5}$) at the AMS 1 monitoring station in May and June 2011 during the episodes of wildland fires expressed as μg N m^{-3}. Fires were denoted when $PM_{2.5}$ concentrations were >25 μg m^{-3}. Daytime concentrations included the 0600–2100 values, while those for nighttime included the 2200–0500 values. Results in each column for a given month followed by different letters indicate significant differences at $\alpha = 0.05$ probability level.

	$N\text{-}NH_3$	N-NO	N-HONO	$N\text{-}NO_2$	$N\text{-}HNO_3$	$N\text{-}NH_4^+$	$N\text{-}NO_3^-$	Total N	$N\text{-}HNO_3$/N-HONO	$PM_{2.5}$
May 2011										
Fire - day	6.02 a	2.59 a	0.16 b	2.84 a	0.30 a	4.80 a	2.42 a	19.29 a	1.88	175.66 a
Fire - night	6.22 a	2.97 a	0.26 a	2.71 a	0.22 b	4.61 a	2.35 a	19.50 a	0.85	187.44 a
No fire - day	0.87 b	2.71 a	0.02 c	1.80 b	0.04 c	1.22 b	0.06 b	6.60 b	2.00	4.36 b
No fire - night	0.82 b	1.98 b	0.02 c	1.16 b	0.03 c	0.89 b	0.04 b	5.00 b	1.50	3.59 b
June 2011										
Fire - day	3.09 a	2.65 b	0.06 b	2.38 a	0.12 a	2.21 a	0.64 a	10.80 a	2.00	60.92 b
Fire - night	2.72 a	4.16 a	0.11 a	2.87 a	0.10 b	2.01 a	0.60 a	11.25 a	0.91	98.66 a
No fire - day	1.53 b	2.03 b	0.02 c	1.43 b	0.06 c	0.83 b	0.05 b	6.13 b	3.00	7.84 c
No fire - night	1.45 b	2.65 b	0.03 c	2.15 ab	0.04 c	0.68 b	0.04 b	7.17 b	1.33	9.52 c

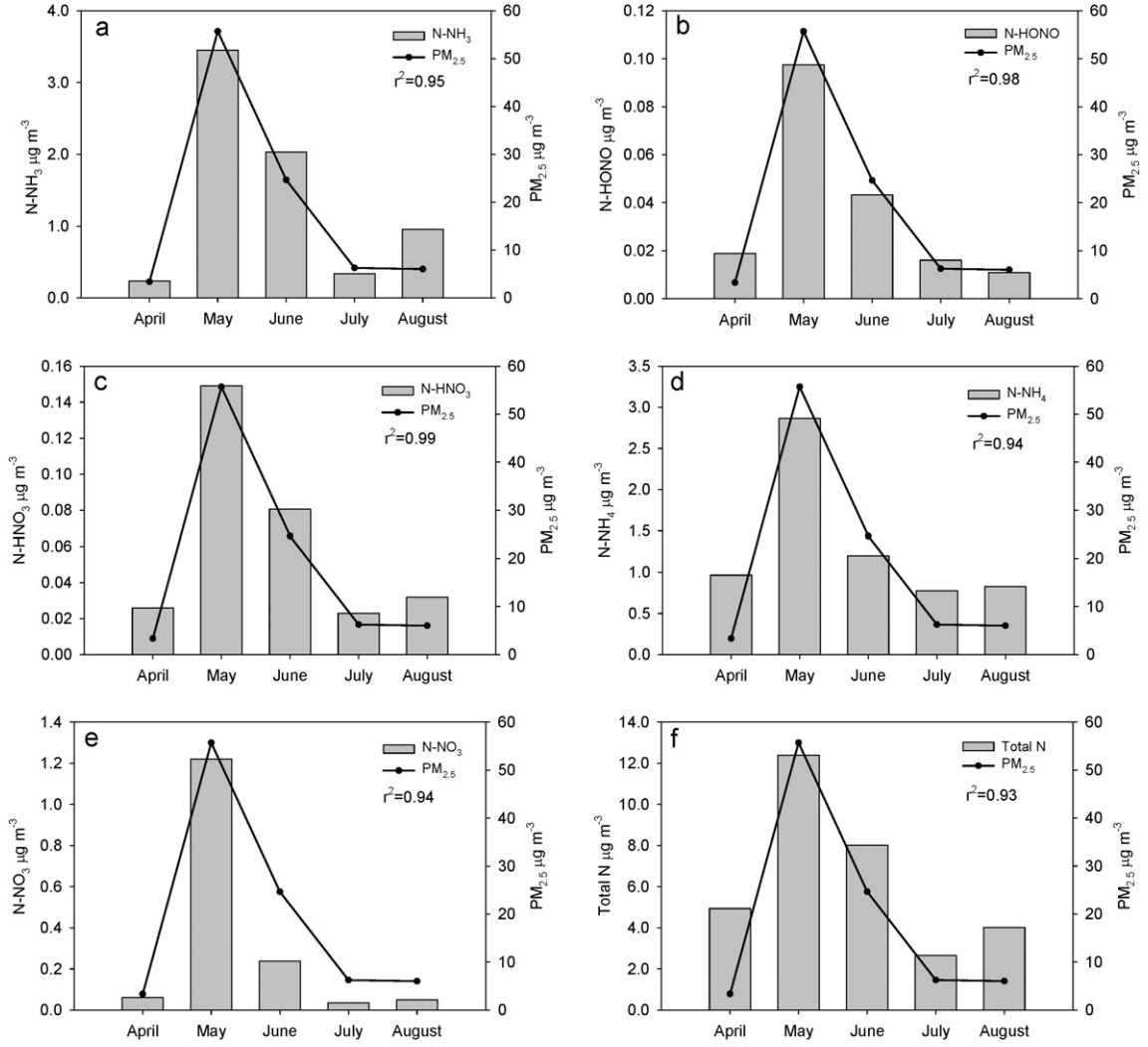

Fig. 7. Correlations between $PM_{2.5}$ and reactive N species measured at the AMS 1 site with the AIM-IC system (monthly means for the April–August 2011 period): a. NH_3; b. HONO; c. HNO_3; d. NH_4^+; e. NO_3^-; f. total inorganic reactive N. Note that the range of values on the left-hand y-axis differs among the six plots.

much higher: in daytime 40.3 fold in May and 12.8 fold in June; and at nighttime 58.8 fold in May and 15.0 fold in June (Table 1).

There was a strong correlation between monthly $PM_{2.5}$ average concentrations and those of NH_3, HONO, HNO_3, NH_4^+, NO_3^- and of total reactive N (Fig. 7a–f). Fires had a strong effect on the apportionment of reactive nitrogenous species (Fig. 8). During the no-fire emission periods in May, NO and NO_2 dominated (40% and 27% in daytime and 40% and 23% at nighttime of total N, respectively). However, during the fire emission periods, the most represented N species were NH_3 and NH_4^+, with 31% and 25% in daytime and 32% and 24% at nighttime, respectively. The NO_3^- contribution to the inorganic N pool was higher during the fire emission periods: 13% for the daytime and 12% for the nighttime compared to 1% during the no-fire emission periods. There was also an increase of HONO to 1% both in daytime and at nighttime, and of HNO_3 to 2% in daytime and no change (1%) at nighttime. In June, during the no-fire emission periods the contribution of NH_3 was higher but that of NH_4^+ lower than in May, while the apportionment of other N species was similar. During the fire periods in June the apportionment of NO and NO_2 was higher, and that of NH_4^+ and NO_3^- lower than in May (Fig. 8).

3.1.3. Other pollutants

At the AMS 1 site, higher O_3 concentrations occurred in daytime and nighttime during the fire emission episodes. The highest O_3 increase occurred in daytime in May: 62.7 ppb during fires vs. 37.4 ppb during the no-fire emission period. No clear trends in changes of SO_2 concentrations related to fire effects were seen and its concentrations were relatively low. The highest concentration was seen in daytime during the fire episodes in June – 5.84 μg S-SO_2 m^{-3}. Concentrations of SO_4^{2-}

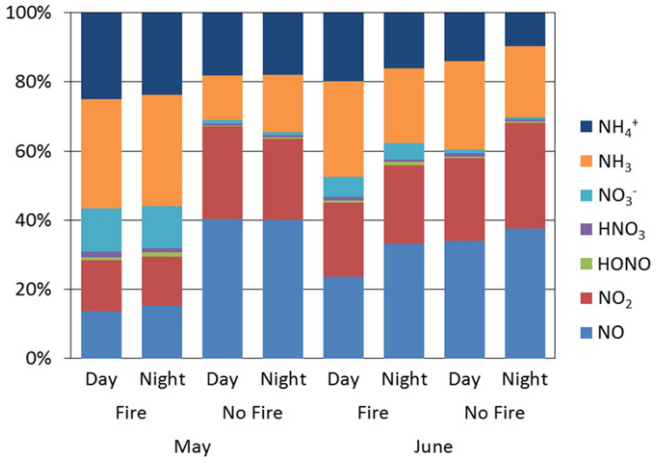

Fig. 8. Apportionment of reactive N species within the inorganic atmospheric N pool in May and June 2011 at the AMS 1 site based on the AIM-IC data.

Table 2
Average concentrations of ozone, sulfur dioxide, and particulate sulfate at the AMS 1 monitoring station in May and June 2011 during the episodes of wildland fires. Fires were denoted when $PM_{2.5}$ concentrations were >25 μg m^{-3}. Daytime concentrations included the 0600–2100 values, while those for nighttime included the 2200–0500 values. Results in each column for a given month followed by different letters indicate significant differences at $\alpha = 0.05$ probability level.

	O_3 (ppb)	S-SO_2 (μg m^{-3})	S-SO_4^{2-} (μg m^{-3})
May 2011			
Fire - day	62.7 a	1.67 ab	1.18 a
Fire - night	36.7 b	1.50 ab	1.06 a
No fire - day	37.4 b	3.38 a	0.98 a
No fire - night	28.5 c	1.27 b	0.40 b
June 2011			
Fire - day	31.4 a	5.84 a	1.29 a
Fire - night	19.7 b	1.11 b	0.79 b
No fire - day	28.6 a	1.57 b	0.45 c
No fire - night	15.6 b	0.62 b	0.33 c

were elevated during the fire emission periods but much less than those for NH_4^+ and NO_3^-. The SO_4-S values increased by 1.2 fold in May and 2.9 in June, while those for the nighttime by 2.7 in May and 2.4 in June (Table 2).

3.2. The AOSR passive sampler monitoring network

Concentrations of air pollutants measured with passive samplers between April 1, 2010 and March 31, 2013 across the AOSR monitoring network are presented as their ranges, means, and medians in Fig. 9. Ammonia showed seasonal cyclical patterns with highest concentrations in summer and lowest in winter (Fig. 9a). No clear seasonal patterns were observed for HNO_3, however there was a pronounced increase of HNO_3 during the 2011 summer fires (Fig. 9b). Nitrogen dioxide and SO_2 concentrations were highest in winter while in summer their concentrations were the lowest (Fig. 9c and d, respectively). There was a strong seasonal pattern of O_3 concentrations with the highest concentrations in April and May, and the lowest values in July and August (Fig. 9e).

3.2.1. Ammonia

During summer 2011, monthly average NH_3 concentrations increased from the lowest values of 2.35 μg N-NH_3 m^{-3} in April (Fig. 10a), to the highest value of 20.3 μg N-NH_3 m^{-3} in June in the network center (Fig. 10c). The maximum NH_3 value (13.4 μg N-NH_3 m^{-3}) was still elevated in July (Fig. 10d) in the central and SW parts of the network. Ammonia concentrations in August (Fig. 10e) decreased

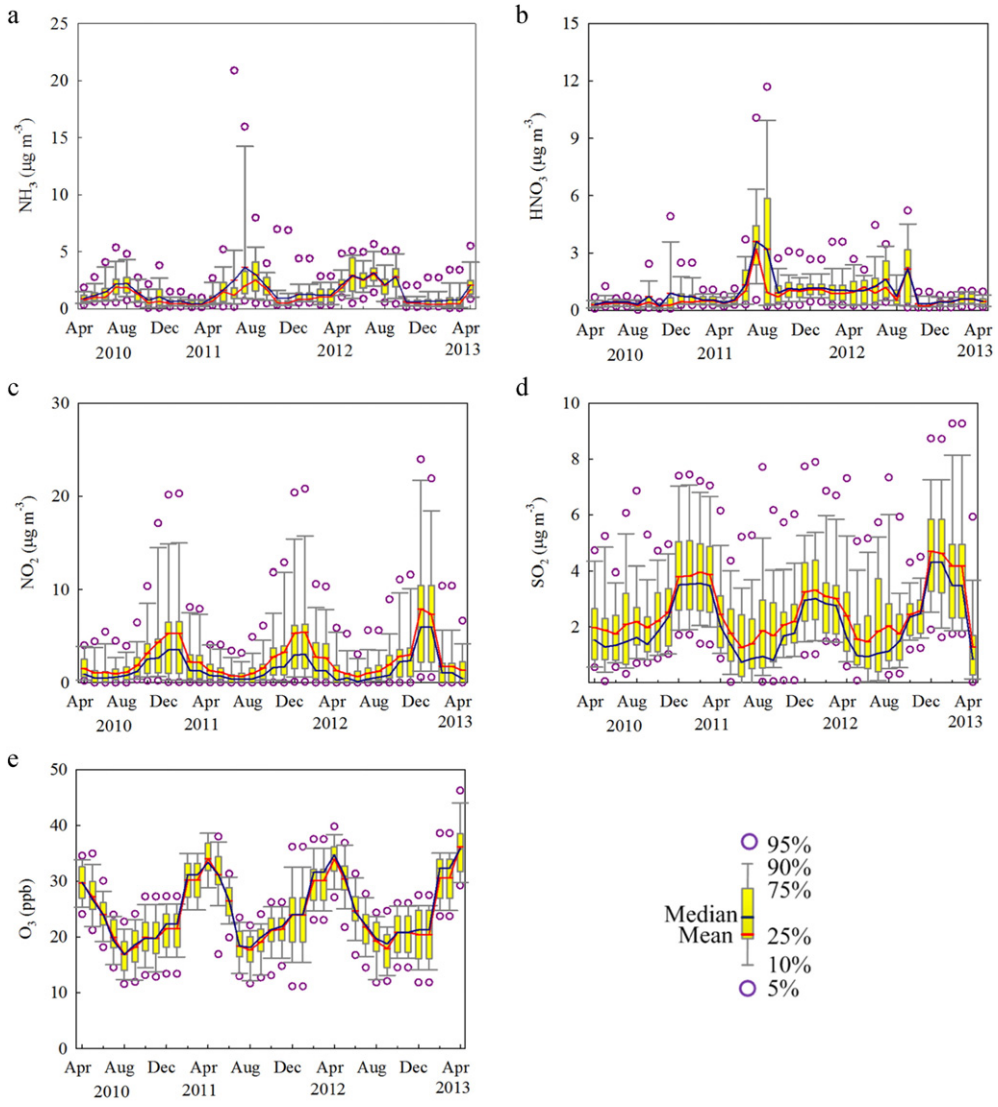

Fig. 9. Concentrations of pollutants measured with passive samplers between April 1, 2010 and March 31, 2013 across the AOSR monitoring network presented as their ranges, means, and medians: a. NH_3; b. HNO_3; c. NO_2; d. SO_2; e. O_3.

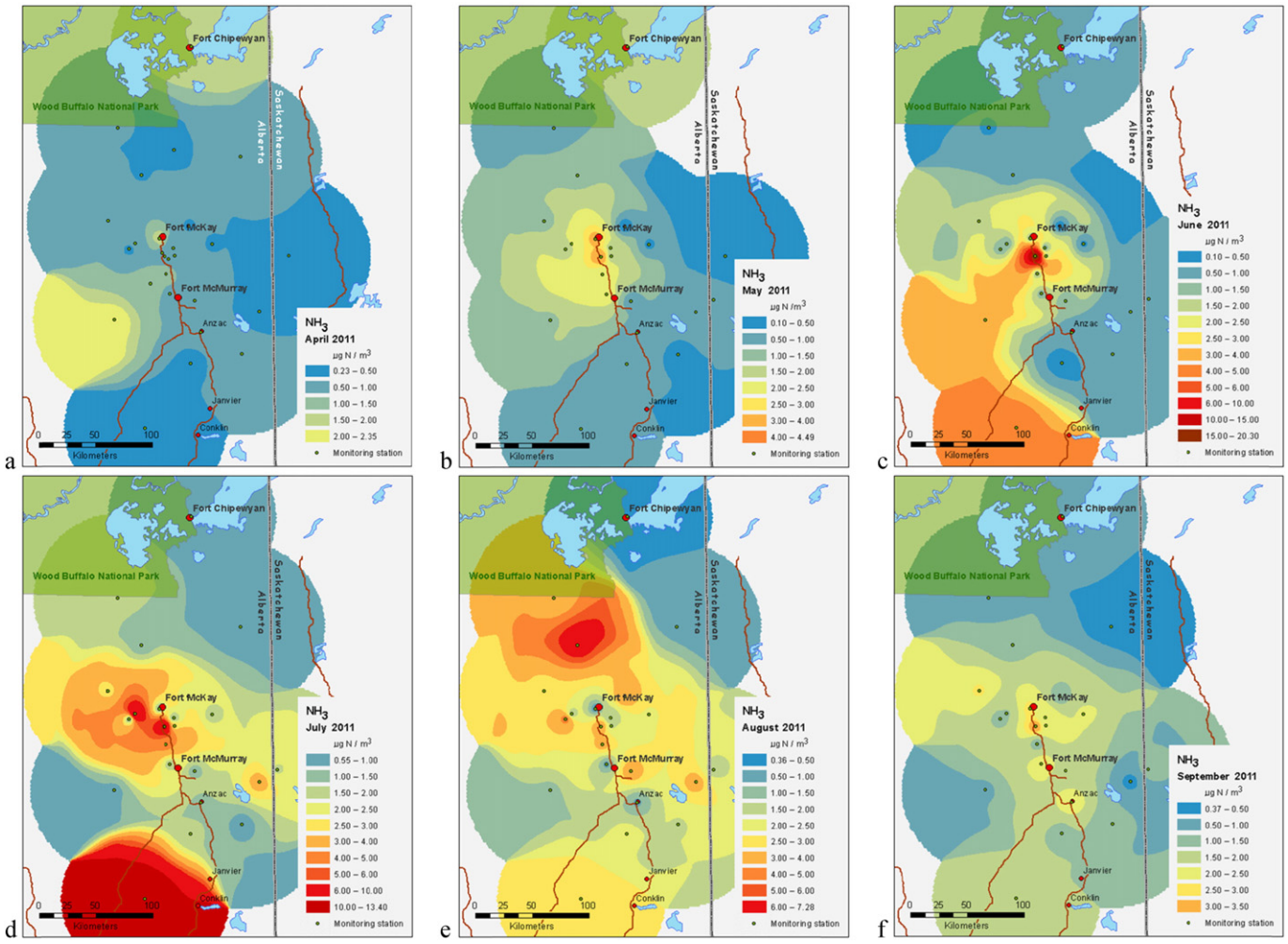

Fig. 10. Spatial distribution of NH_3 concentrations on the AOSR monitoring network presented as monthly means in summer 2011: a. April; b. May; c. June; d. July; e. August; f. September.

with a maximum of 7.28 µg N-NH_3 m^{-3} reached in the NW of the AOSR near the Richardson Fire perimeter. In September, NH_3 concentrations significantly decreased (maximum ~3.5 µg N-NH_3 m^{-3}) and the most elevated values during this time were widely dispersed over the entire monitoring area (Fig. 10f).

Generally, NH_3 concentrations were higher in summer than in winter during the 2010–2012 monitoring period (Fig. 11a–f). Summer season concentrations were the highest in 2011 with a maximum value of 7.66 µg N-NH_3 m^{-3} observed in the center of the AOSR between Fort McKay and Fort McMurray. In summer 2011, elevated NH_3 concentrations (~3–4 µg N-NH_3 m^{-3}) were also found in the SW portion of the monitoring area (Fig. 11b). The maximum network values in summers 2010 and 2012 found in the AOSR center were about 2-fold lower than those in 2011 (Fig. 11a, and c, respectively). In 2012, similar to 2011, elevated NH_3 concentrations were also observed in the SW part of the AOSR (Fig. 11c). The winter values were higher for the entire area in 2011 (Fig. 11e) compared to those in 2010 (Fig. 11d) and 2012 (Fig. 11f) and the highest NH_3 concentrations occurred in the AOSR center.

3.2.2. Nitric acid

During summer 2011, maximum HNO_3 concentrations were gradually increasing from very low values (<0.27 µg N-HNO_3 m^{-3}) in April and May (Fig. 12a, b), to elevated concentrations in June reaching 0.91 µg N-HNO_3 m^{-3} in the central and NW portions of the AOSR (Fig. 12c), and very high values reaching 2.58 µg N-HNO_3 m^3 over the entire AOSR in July (Fig. 12d), and its eastern part in August (Fig. 12e). Concentrations of HNO_3 were much lower in September reaching 0.61 µg N-HNO_3 m^{-3} in the central part of the AOSR near the Richardson Fire perimeter (Fig. 12f).

The 2011 summer concentrations were the highest among the monitoring seasons with a seasonal maximum mean reaching 0.74 µg N-HNO_3 m^{-3} in the central and NE portions of the AOSR (Fig. 13b), while the maximum network values in the 2010 and 2012 summers were about 3- and 2-fold lower, respectively (Fig. 13a, c). While the 2010 winter HNO_3 concentrations (Fig. 13d) were similar to those in the 2010 summer (Fig. 13a), the 2011–2012 winter concentrations (Fig. 13e and f) were lower than in summers of the respective years. Among the three winter periods, the 2011 winter values were the highest (Fig. 13e).

3.2.3. Other pollutants

Higher monthly NO_2 and SO_2 concentrations occurred in winter than in summer (Fig. 9c and d). The highest winter mean NO_2 concentrations for the entire network were ~5.0 µg m^{-3} in 2010, 5.1 µg m^{-3} in 2011, and 7.8 µg m^{-3} in 2012. The lowest NO_2 values were observed in midsummer with their means ~1 µg m^{-3}. The winter NO_2 means for individual sites exceeded 20 µg m^{-3} each year, with the highest value of ~24.5 µg m^{-3} recorded in 2012 (Fig. 9c). The highest network SO_2 means for winter were 3.9 µg m^{-3} in 2010, 3.2 µg m^{-3} in 2011, and 4.7 µg m^{-3} in 2012. Highest winter SO_2 means for individual sites exceeded 7.0 µg m^{-3} each year, with the highest value of ~9.5 µg m^{-3}

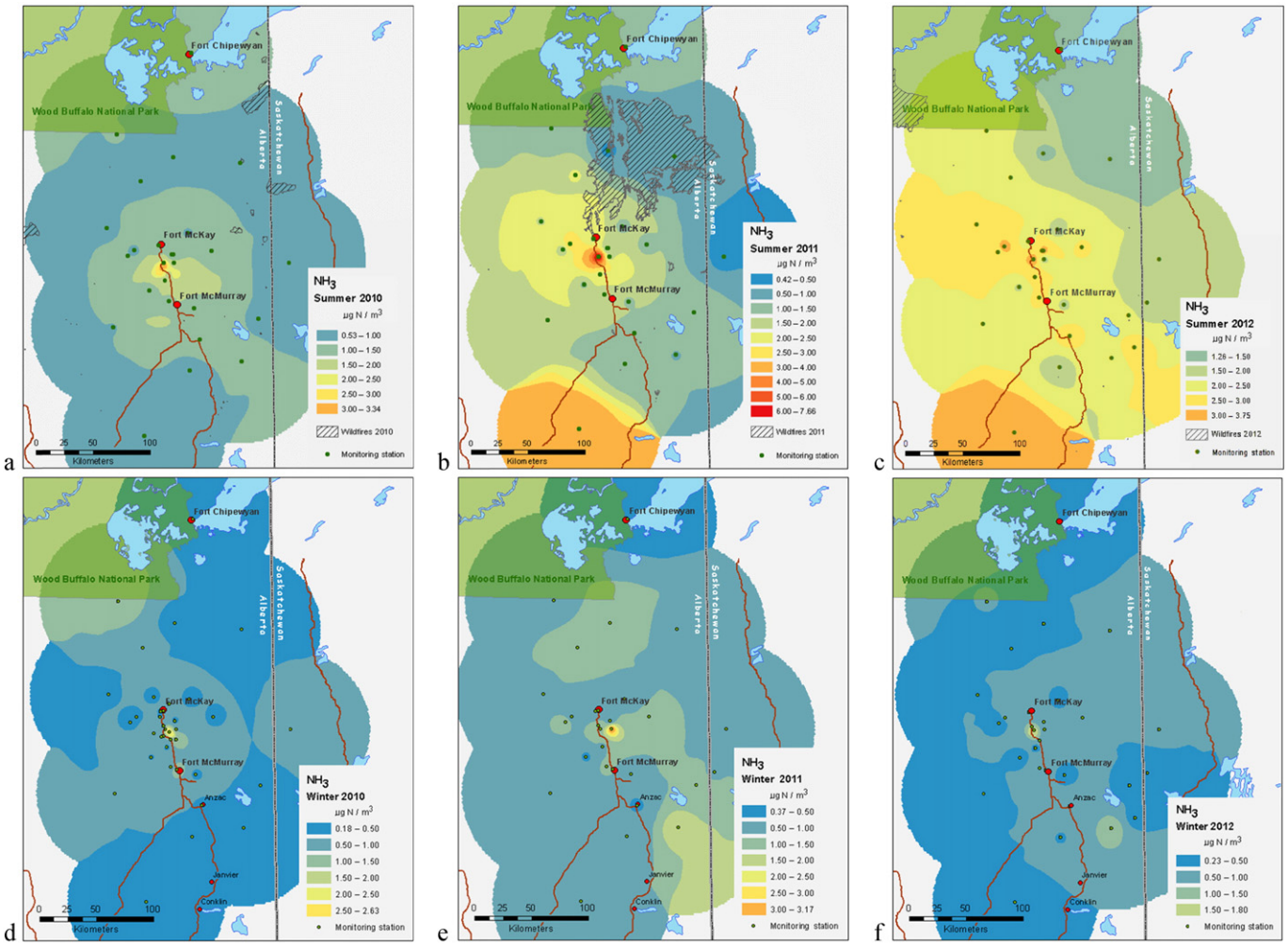

Fig. 11. Spatial distribution of NH_3 concentrations on the AOSR monitoring network presented as seasonal means: a. summer 2010; b. summer 2011; c. summer 2012; d. winter 2010; e. winter 2011; f. winter 2012.

in 2012 (Fig. 9d). The lowest SO_2 means were in mid-summer - 1.7, 1.2 and 1.5 µg m^{-3} in 2010, 2011 and 2012, respectively. The highest O_3 concentrations occurred in April with network mean values between 30 and 36 ppb for April over the monitoring period. The lowest O_3 concentrations were in August with the network means as low as 17 ppb in 2010 and 18 ppb in 2011 and 2012 (Fig. 9e). Contrary to NH_3 and HNO_3, monthly concentrations of NO_2, SO_2 and O_3 for the entire network did not increase during the 2011 summer wildfires (Fig. 9c, d, e).

4. Discussion

4.1. Changes in air chemistry

4.1.1. Fine particulate matter ($PM_{2.5}$)

After carbon dioxide (CO_2) and carbon monoxide (CO), fine particulate matter ($PM_{2.5}$) provides most of the wildland fire emissions mass (Urbanski et al., 2009). Ambient concentrations of $PM_{2.5}$ increase with wildland fires emissions (Goldammer et al., 2009; Urbanski et al., 2009) and have been used as an important indicator of air quality changes caused by wildland fires (Schweizer and Cisneros, 2014). Very high $PM_{2.5}$ concentrations at the AMS 1 receptor site occurred when air masses were coming from the north after sweeping over the fire-affected area. These hourly concentrations exceeding 450 µg m^{-3} were much higher than the highest concentration of 214 µg m^{-3} recorded downwind of the 2013 Aspen Fire in the Sierra Nevada Mountains of California (Burley et al., in press). The 24-h average concentrations reaching 368 µg m^{-3} at the AMS 1 receptor greatly exceeded the maximum values of ~163 µg m^{-3} recorded during the 2006/2007 bush fires in Victoria, Australia (Haikerwal et al., 2015) or ~170 µg m^{-3} measured during high air pollution episodes in Beijing, China (Zheng et al., 2005). In this context it should be noted that average $PM_{2.5}$ concentrations calculated in our study were quite likely underestimated because of the 450 µg m^{-3} limit set for the monitoring instrument. The highest $PM_{2.5}$ levels occurred in the second half of May due to the close proximity of very intense and rapidly expanding fires. Judging from the backward trajectories moving over the fire-affected area, we estimate that the age of smoke plumes reaching the receptor site in the initial phase of the Richardson Fire are within the range of a few to several hours (Fig. 3). These very high $PM_{2.5}$ levels started diminishing in June when the fires moved further away from the receptor site in a NE direction. While carbon aerosols, consisting of elemental carbon (soot) and organic carbon particles make up most of the $PM_{2.5}$ in smoke from wildland fires, particulate NH_4^+ and NO_3^- are important inorganic components present mainly as NH_4NO_3 and $(NH_4)_2SO_4$ (Urbanski et al., 2009; Goldammer et al., 2009; Hyde et al., 2016). In the absence of fire emissions, the relative contribution of these nitrogenous compounds to ambient $PM_{2.5}$ increases <http://www3.epa.gov/airtrends/aqtrnd04/pmreport03/pmunderstand_2405.pdf>. After the outbreak of the Richardson Fire on May 15th, concentrations of NH_4^+ and NO_3^- were strongly correlated with the $PM_{2.5}$ changes. Although concentrations of SO_4^{2-} also increased during the fire smoke episodes, they were much less correlated with the $PM_{2.5}$ increases indicating

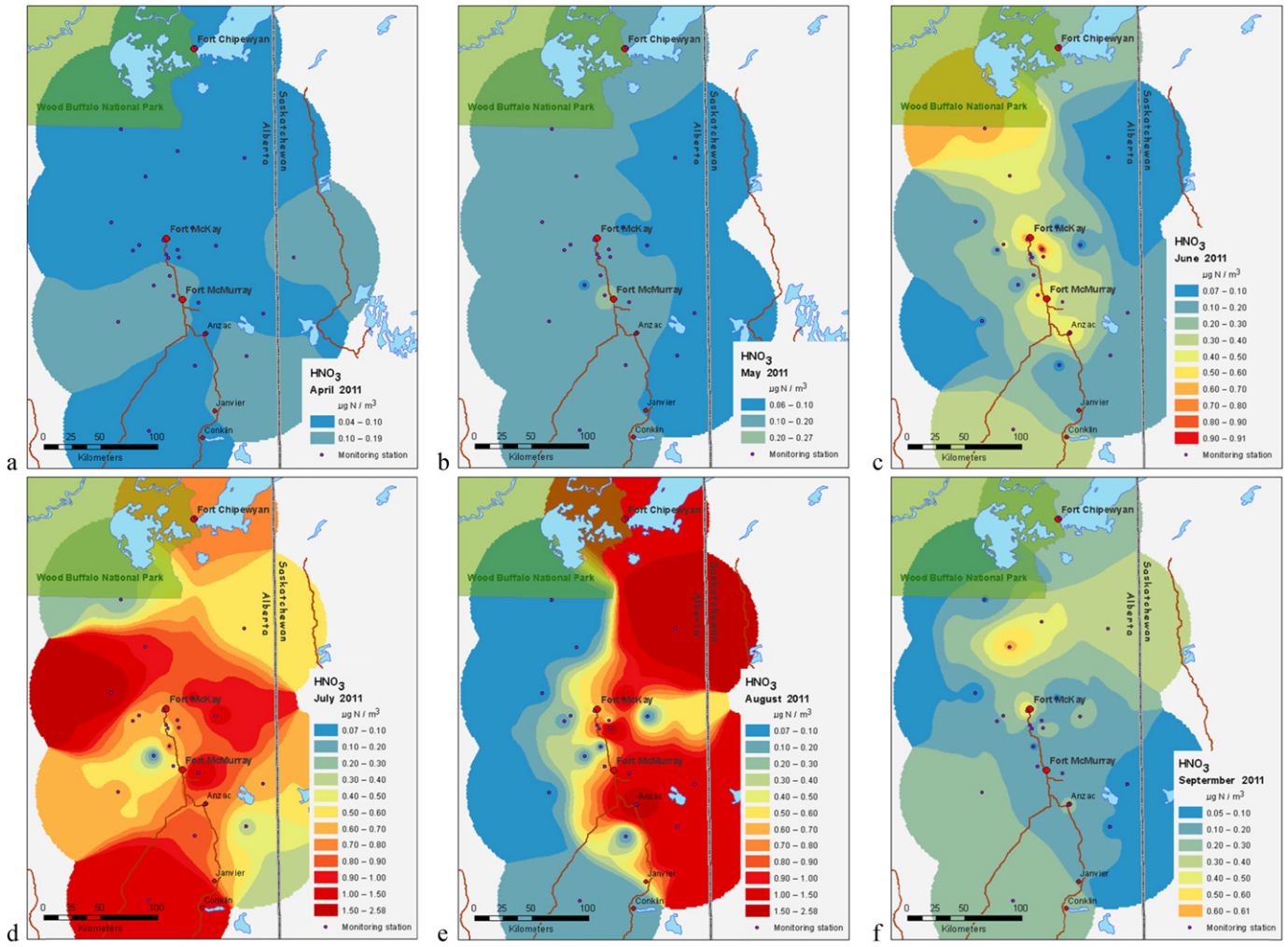

Fig. 12. Spatial distribution of HNO_3 concentrations on the AOSR monitoring network presented as monthly means in summer 2011: a. April; b. May; c. June; d. July; e. August; f. September.

another emission source for SO_4^{2-}. Our results confirm that NH_4NO_3, and to a lesser degree $(NH_4)_2SO_4$, were important components of $PM_{2.5}$ during the fire emission periods and that their concentrations increased with the intensity of fires as indicated by higher $PM_{2.5}$ concentrations. We observed a much higher apportionment of NH_4^+ and NO_3^- among the inorganic N components during more intense fires in May compared to those in June. Although absolute concentrations of NH_4^+ and NO_3^- increased during the fire emission episodes, their relative contribution to $PM_{2.5}$ was much lower than during the no-fire emission periods because of the dominance of carbon aerosols <http://www3.epa.gov/airtrends/aqtrnd04/pmreport03/pmunderstand_2405.pdf>.

4.1.2. Gaseous and particulate nitrogenous species

Analysis of the May – June 2011 data from the AMS 1 site showed large differences in gaseous and particulate N pollutants during the no-fire emission and fire emission periods. Absolute concentrations of all measured N species except NO increased during the fire emission episodes. The observed changes in NH_3, HONO, HNO_3, NH_4^+ and NO_3^- concentrations during fire emissions were highly correlated with fire intensity as indicated by the $PM_{2.5}$ concentrations. There were large differences in the relative contribution of various N compounds to total inorganic N between the no-fire emission and fire emission periods, especially in May. While in the absence of fires, NO and NO_2 dominated the inorganic N fraction, their relative share during the fires was reduced by ~3 fold mainly due to the increased contribution of NH_3 (~2 fold), NH_4^+ (~1.4 fold), and NO_3^- (~13 fold) (daytime, May). While concentrations of HONO and HNO_3 greatly increased during the fires (~8 fold), their contribution to the total inorganic N was relatively small at approximately 1% for each gas.

High levels of the reduced forms of N, NH_3 and NH_4^+, and their dominance in the pool of inorganic N pollutants, occurred from the very beginning of the Richardson Fire. This is an indication of their presence already in the flaming phase of combustion, not only during the smoldering phase of fires as previously reported (Goldammer et al., 2009). Concentrations of HONO and HNO_3 increased as the emissions intensified. In typical summer conditions (high temperatures and solar radiation) and in the absence of fires, HNO_3 dominates over HONO (Acker et al., 2005; Bytnerowicz et al., 2002). However, in areas affected by wildland fires, increased HONO concentrations have been reported (Burling et al., 2011; Bytnerowicz et al., 2002; Lammel and Cape, 1996) and were most likely caused by a rapid chemical reduction of NO_2 released from fires to HONO on soot particles in smoke plumes (Kalberer et al., 1999). This phenomenon can explain the presence of elevated HONO concentrations at the AMS 1 site at night when conditions were favorable for its generation. On the other hand, conditions favoring oxidation of HONO may explain higher HNO_3 levels in the daytime. Elevated HNO_3 concentrations in biomass smoke plumes have been reported previously (LeBel et al., 1988).

4.1.3. Other pollutants

There was no obvious increase of SO_2 concentrations during the fires except the daytime increase in June. These results confirm that SO_x emissions from fires are typically low (Goldammer et al., 2009). The

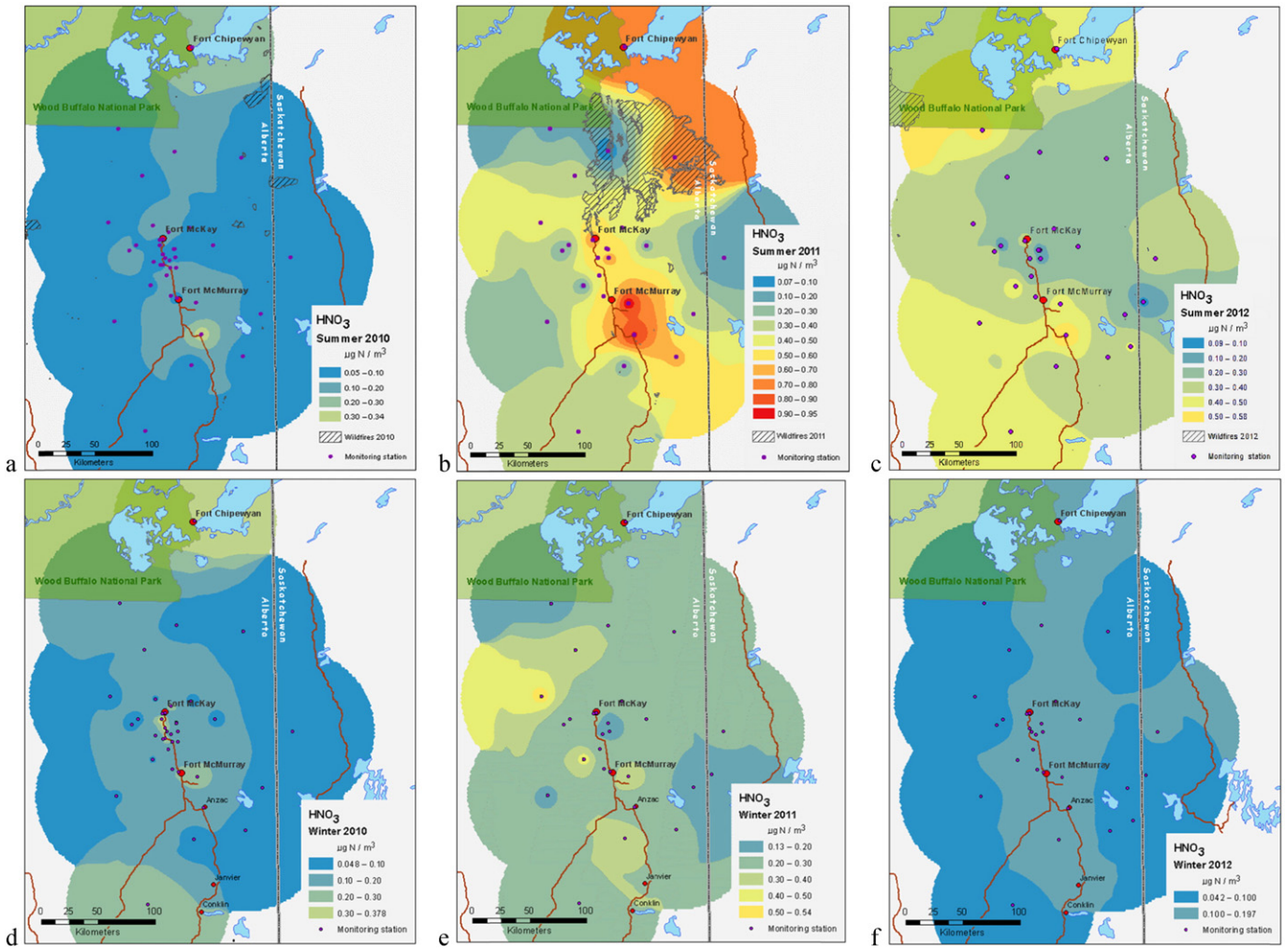

Fig. 13. Spatial distribution of HNO_3 concentrations on the AOSR monitoring network presented as seasonal means: a. summer 2010; b. summer 2011; c. summer 2012; d. winter 2010; e. winter 2011; f. winter 2012.

elevated concentrations of $S\text{-}SO_4^{2-}$ observed during the fires were from a local stack emission (Hsu and Clair, 2015).

Daytime O_3 concentrations measured with an active monitor in the AOSR center during the fire emission episodes in May 2011 were much higher than those during the no-fire emission periods. However, in June 2011, also during the fire emission periods, O_3 concentrations were only slightly higher than during the no-fire emission periods. Elevated O_3 concentrations in wildland fire smoke have been reported, and chemical reactions leading to generation of O_3 are complex (Delany et al., 1985; Urbanski et al., 2009). Ambient O_3 concentrations near wildland fires depend on many factors, such as distance and direction from the fire, presence of NO_x and VOCs in the smoke plume and kinetics of their reactions, as well as meteorological conditions such as wind direction, temperature or solar radiation (Delany et al., 1985). Elevated O_3 concentrations have been found downwind of large wildland fires in the western U.S. (Jaffe et al., 2008; Jaffe and Wigder, 2012) and in southern California downwind of the 2007 San Diego wildland fires (Bytnerowicz et al., 2010a). However, no increase in O_3 concentrations were detected in the immediate vicinity of wildland fires in the central Sierra Nevada in California (Bytnerowicz et al., 2013). Similarly, studies in boreal regions have shown no changes, or even diminished ambient O_3, downwind of fires due to low mixing ratios of NO_x, sequestration of NO to peroxyacetyl nitrate, and reduction of photochemical processes due to aerosol effects (Jaffe and Wigder, 2012).

Ozone concentrations over the entire AOSR passive sampling network were generally low and did not increase during the 2011 wildland fires. These findings seem to confirm the trends described above for boreal regions (Jaffe and Wigder, 2012). During the entire period reported in this study results from passive samplers showed regularly occurring seasonal O_3 cycles. The highest O_3 concentration occurred in April, while the lowest values were observed in the middle of summer (July – September). This pattern is typical for high latitude remote locations in the northern Hemisphere (Lin et al., 2014; Pruchniewicz, 1973; Singh et al., 1978). Late spring stratospheric intrusions could be responsible for increased ozone on some days, especially when the polar jet stream moves southwards over southern Canada and the western U.S. This has been reported to occur following strong La Niña winters (Lin et al., 2015). However, ozone concentrations measured at AOSR sites were much lower compared to rural sites in the western U.S. (Cooper et al., 2011). The seasonal patterns in the AOSR are different from patterns reported from locations at lower latitudes. In lower latitude locations the O_3 maxima occur later in the year – typically in May and during the summer months when ambient conditions promote higher rates of photochemical reactions (Cooper et al., 2014; Oltmans et al., 2013; The Royal Society, 2008). Decreasing O_3 concentrations in the middle of summer at AOSR sites could be caused by its deposition to forest canopies (Rannick et al., 2012) and also because of the seasonal minimum of the stratospheric influence.

4.2. Spatial distribution of pollutants in the AOSR

Information on monthly concentrations of NH_3, HNO_3, NO_2, SO_2 and O_3 obtained from a network of passive samplers made evaluation of the temporal and spatial changes for these pollutants possible. In general, spatial and temporal patterns for NO_2, SO_2 and O_3 did not change significantly as a result of the 2011 wildland fires (Hsu et al., 2016). However, the summer 2011 fires strongly affected the spatial distribution of NH_3 and HNO_3. Such changes were seen for individual months during summer 2011. Changes were also observed for the summer and winter seasons of 2011 when compared to those of 2010 and 2012.

4.2.1. Ammonia

While in April 2011 NH_3 concentrations were very low, in the subsequent months they gradually increased. An initial increase in May and highly elevated levels in June was mostly seen in the center of the AOSR and included the AMS 1 monitoring site. This increase was most likely caused by the smoke emissions moving south with the prevailing winds from the nearby Richardson Fire north of Fort McKay. Effects of the Richardson Fire were still seen in July in a large area west of Fort McKay. In August, an extensive area north of Fort McKay experienced elevated NH_3 most likely caused by the smoldering phase of fires. In September much lower levels of NH_3 were observed over the entire AOSR indicating diminishing effects of fire emissions. High NH_3 concentrations in June and July occurring in the southern portion of the AOSR were most likely due to transport of the pollutant from the south. These high NH_3 concentrations were probably not related to fire emissions or oil processing activities but rather to long-range transport of NH_3 from agricultural and urban activities in the Edmonton agglomeration and the Grand Prairie/Peace River farmland driven by the prevailing SW and W winds typical for the summer conditions (http://www1.agric.gov.ab.ca/$department/deptdocs.nsf/all/sag6452/$FILE/onl_s_19_twp_annual_normals_19712000.gif). These trends were similar in summer 2012 although with lower maximum concentrations in the AOSR center. For the entire AOSR, the lowest NH_3 levels were in 2010.

Our results seem to confirm that in dry summer conditions NH_3 can be transported a long distance from the pollution-source areas. This has already been shown for the eastern parts of the Sierra Nevada Mountains affected by agricultural emissions from the Central Valley of California (Bytnerowicz et al., 2016). High NH_3 concentrations in the southern portion of AOSR were not observed during winter in the absence of agricultural activities in the Edmonton area. During wintertime, elevated NH_3 levels were limited to the AOSR industrial center.

4.2.2. Nitric acid

Very low HNO_3 concentrations were recorded in April and May 2011. Elevated HNO_3 at the AMS 1 site during the fire periods in May as reported above apparently had little effect on the monthly mean measured with passive samplers in the entire AOSR monitoring network. However, increases in HNO_3 concentrations in the AOSR began in June due to the impacts of the Richardson Fire emissions. In June, elevated HNO_3 concentrations were mostly seen at the AOSR center, while in July the entire AOSR experienced very high HNO_3 concentrations. In August, elevated HNO_3 levels were mostly limited to the eastern portion of AOSR. In September, only slightly elevated HNO_3 concentrations were seen in the immediate vicinity of the Richardson Fire in the northern portion of the study domain.

As observed for NH_3, the lowest summer season HNO_3 concentrations occurred in 2010, while the highest levels were detected in summer 2011 near the Richardson Fire perimeter. These high HNO_3 summer mean concentrations resulted from the highly elevated monthly concentrations. In winters 2010 and 2012, HNO_3 levels were very low, while those in 2011 were slightly higher, especially near the Richardson Fire area. A lack of clear differences between the summer and winter season was typical for the entire 2005–2013 monitoring period at the AOSR (Hsu and Bytnerowicz, 2015).

4.3. Ecological and human health impacts of changes in air chemistry caused by the Richardson Fire

During the most intensive phase of the Richardson Fire from mid-May until the end of June 2011 $PM_{2.5}$ concentrations reached very high hourly values, >450 μg m^{-3}. The 24 h concentrations exceeded the U.S. NAAQS of 35 μg m^{-3} and the Canadian CWS of 30 μg m^{-3} during 13 days in May and 7 days in June. Concentrations of O_3, NO_2, and other criteria air pollutants, were low during the entire monitoring period and did not exceed the U.S. NAAQS standards <http://www3.epa.gov/ttn/naaqs/criteria.html>. The Alberta Ambient Air Quality Objective (AAAQO) of 82 ppb of O_3 for 1 h was exceeded 8 times at AMS 1 in 2011, all exceedances occurring during the Richardson Fire. The 1-h AAAQO of 159 ppb for NO_2 was not exceeded in 2011 (WBEA, 2012).

While elevated concentrations of NH_3 and HNO_3 were below levels potentially toxic to plants (Bytnerowicz et al., 1998), they contributed to increased deposition of inorganic N in the AOSR. Modeled dry deposition fluxes at AMS 1 that were based on atmospheric concentrations of nitrogenous pollutants measured at the site indicate that N dry deposition increased as a result of fire emissions. The most dramatic increase occurred in the case of HNO_3 when deposition in summer 2011 was 2–4 times greater than in summers 2008–2010 (Hsu et al., 2016). Absolute values for deposition of particulate NO_3^- were much lower than for HNO_3, but in summer 2011 deposition of particulate NO_3^- was orders of magnitude greater than the previous summers. In the case of reduced forms of N, deposition of NH_3 and NH_4^+ were 1.3–2.5 and 2–3 times greater in summer 2011 compared to the previous three summers. Dry deposition of SO_2 did not change during the 2011 fires, while deposition of particulate SO_4^{-2} doubled in summer 2011 (Hsu et al., 2016).

Total summertime N deposition (wet + dry) at AMS 1 in summers 2008 to 2010 averaged ~1.5 kg ha^{-1} yr^{-1} compared to ~2.5 kg ha^{-1} yr^{-1} during summer 2011 (Hsu et al., 2016), the season affected by the Richardson Fire. While the relative increase in N deposition in summer 2011 is quite large compared to previous summers, the absolute increase in estimated N deposition (~1.0 kg N ha^{-1} yr^{-1}) is small and not likely to be highly significant in terms of ecological effects. Throughfall measurements at AMS 1 with ion exchange resin samplers did not detect an increase in N or S deposition in summer 2011 (Fenn et al., 2015). A possible reason why this increase in dry deposition was not observed in throughfall is because the increased deposition was not large and much of the deposition may have been retained by the canopy and not collected as throughfall. This is a reasonable explanation considering that most of the increased N deposition as a result of the fire was in the form of the highly reactive pollutant HNO_3.

5. Conclusions

5.1. The 2011 northern Alberta Richardson Fire resulted in very high $PM_{2.5}$ concentrations at the AOSR receptor site located in Fort McKay. Hourly $PM_{2.5}$ concentrations in May were >450 μg m^{-3} and the NAAQS of 35 μg m^{-3} and CWS of 30 μg m^{-3} were exceeded on 20 days in May and June.

5.2. During the fire emission events, there was a sharp increase in NH_3, HONO, HNO_3, NH_4^+, NO_3^- and total inorganic reactive N concentrations which were closely correlated with $PM_{2.5}$ concentrations.

5.3. There were large differences in the relative contribution of various N compounds to total inorganic N between the no-fire emission and fire emission periods. While in the absence of fire emissions, NO and NO_2 dominated, their relative contribution during fire emissions was ~3 fold smaller. That decrease was mainly due to the increased contribution of NH_3, NH_4^+ and NO_3^-. While concentrations of HONO and HNO_3 also greatly increased

during fire emission periods, their contribution to the total inorganic N pool was relatively small.

5.4. High concentrations of NH_3 and NH_4^+ and their dominance in the pool of inorganic N pollutants occurred from the beginning of the Richardson Fire indicating their presence already in the flaming phase of combustion. Previous studies indicated that NH_3 emissions occurred primarily in the fire smoldering phase.

5.5. Elevated NH_3 and HNO_3 concentrations occurred over large areas of northern Alberta during the Richardson Fire. While their concentrations were not toxic to plants, due to their high deposition velocities these gases contributed to increased atmospheric N deposition to the forest ecosystems in the AOSR.

5.6. Generally, no significant differences in O_3 and SO_2 concentrations were observed between the fire and no-fire periods, and their levels were not harmful to human health or sensitive vegetation. An exception were the elevated O_3 concentrations in the vicinity of the AMS 1 site in May 2011 with potential negative effects on people and ecosystems.

Acknowledgements

This work was funded by the Wood Buffalo Environmental Association (WBEA), Fort McMurray, Alberta, Canada (Agreement numbers NRMG-11-CO-11272139-025 and 06-CO-11272172-005). The authors thank WBEA members and staff for assistance with field monitoring activities and other means of support for this study. Comments from Drs. Owen Cooper and Meiyun Lin on early versions of the manuscript are greatly appreciated. The content and opinions expressed by the authors in this article do not necessarily reflect the views of the WBEA and its members. The authors gratefully acknowledge the NOAA Air Resources Laboratory (ARL) for the provision of the HYSPLIT transport and dispersion model and/or READY website (http://www.ready.noaa.gov) used in this publication.

Appendix A. Supplementary data

Supplementary data to this article can be found online at http://dx.doi.org/10.1016/j.scitotenv.2016.07.052.

References

Acker, K., Möller, D., Auel, R., Wieprecht, Kalass, D.K., 2005. Concentrations of nitrous acid, nitric acid, nitrite and nitrate in the gas and aerosol phase at a site in the emission zone during ESCOMPTE 2001 experiment. Atmos. Res. 74, 507–524.

Akagi, S.K., Craven, J.S., Taylor, J.W., McMeeking, G.R., Yokelson, R.J., Burling, I.R., Urbanski, S.P., Wold, C.E., Seinfeld, J.H., Coe, H., Alvarado, M.J., Weise, D.R., 2012. Evolution of trace gases and particles emitted by a chaparral fire in California. Atmos. Chem. Phys. 12, 1397–1421.

Andreae, M.O., Merlet, P., 2001. Emission of trace gases and aerosols from biomass burning. Glob. Biogeochem. Cycles 15, 955–966.

Burley, J.D., Bytnerowicz, A., Buhler, M., Zielinska, B., Schweizer, D., Cisneros, R., Schilling, S., Chapman Varela, F., McDaniel, M., Horn, M., Dulen, D., 2016. Air Quality at Devils Postpile National Monument, Sierra Nevada Mountains, California, USA. Aerosol Air Qual. Res. (in press).

Burling, I.R., Yokelson, R.J., Akagi, S.K., Urbanski, S.P., Wold, C.E., Griffith, D.W.T., Johnson, T.J., Reardon, J., Weise, D.R., 2011. Airborne and ground-based measurements of the trace gases and particles emitted by prescribed fires in the United States. Atmos. Chem. Phys. 11, 12197–12216.

Bytnerowicz, A., Dueck, T., Godzik, S., 1998. Nitric oxide, nitrogen dioxide, nitric acid vapor and ammonia. In: Flagler, R. (Ed.), Recognition of Air Pollution Injury to Vegetation: A Pictorial Atlas. Air & Waste Management Association, Pittsburgh, PA (5–1 through 5–17).

Bytnerowicz, A., Carroll, J.J., Takemoto, B.K., Miller, P.R., Fenn, M.E., Musselman, R.C., 2000. Distribution and transport of air pollutants to vulnerable California ecosystems. In: Scow, K.M., Fogg, G.E., Hinton, D.E., Johnson, M.L. (Eds.), Integrated Assessment of Ecosystem Health. Lewis Publishers, Baca Raton, pp. 93–118.

Bytnerowicz, A., Tausz, M., Alonso, R., Jones, D., Johnson, R., Grulke, N., 2002. Summertime distribution of air pollutants in Sequoia National Park, California. Environ. Pollut. 118, 187–203.

Bytnerowicz, A., Sanz, M.J., Arbaugh, M.J., Padgett, P.E., Jones, D.P., Davila, A., 2005. Passive sampler for monitoring ambient nitric acid (HNO_3) and nitrous acid (HNO_2) concentrations. Atmos. Environ. 39, 2655–2660.

Bytnerowicz, A., Omasa, K., Paoletti, E., 2007. Integrated effects of air pollution and climate change on forests: a northern hemisphere perspective. Environ. Pollut. 147, 438–445.

Bytnerowicz, A., Cayan, D., Riggan, P., Schilling, S., Dawson, P., Tyree, M., Wolden, L., Tissell, R., Preisler, H., 2010a. Analysis of the effects of combustion emissions and Santa Ana winds on ambient ozone during the October 2007 southern California wildfires. Atmos. Environ. 44, 678–687.

Bytnerowicz, A., Frączek, W., Schilling, S., Alexander, D., 2010b. Spatial and temporal distribution of ambient nitric acid and ammonia in the Athabasca Oil Sands Region, Alberta. J. Limnol. 69 (Suppl. 1), 11–21. http://dx.doi.org/10.3274/JL10-69-S1-03.

Bytnerowicz, A., Burley, J.D., Cisneros, R., Preisler, H.K., Schilling, S., Schweizer, D., Ray, J., Dullen, D., Beck, C., Auble, B., 2013. Surface ozone at the Devils Postpile National Monument receptor site during low and high wildland fire years. Atmos. Environ. 65, 129–141.

Bytnerowicz, A., Fenn, M., Allen, E.B., Cisneros, R., 2016. Atmospheric chemistry. In: Mooney, H., Zavaleta, E. (Eds.), Ecosystems of California. University of California Press, Oakland, pp. 107–128.

Carslaw, D.C., Ropkins, K., 2016. Openair: Open-Source Tools for the Analysis of Air Pollution Data. R package version 1.8–6, <URL http://CRAN.R-project.org/package=openair>.

Conard, S.G., Ivanova, G.A., 1998. Wildfire in Russian boreal forests - potential impacts of fire regime characteristics on emission and global carbon balance estimates. Environ. Pollut. 98, 305–313.

Cooper, O.R., Oltmans, S.J., Johnson, B.J., Brioude, J., Angevine, W., Trainer, M., Parrish, D.D., Ryerson, T.R., Pollack, I., Cullis, P.D., Ives, M.A., Tarasick, D.W., Al-Saadi, J., Stajner, I., 2011. Measurement of western U.S. baseline ozone from the surface to the tropopause and assessment of downwind impact regions. J. Geophys. Res. 116, D00V03. http://dx.doi.org/10.1029/2011JD016095.

Cooper, O.R., Parrish, D.D., Ziemke, J., Balashov, N.V., Cupeiro, M., Galbally, I.E., Gilge, S., Horowitz, L., Jensen, N.R., Lamarque, J.-F., Naik, V., Oltmans, S.J., Schwab, J., Shindell, D.T., Thompson, A.M., Thuret, V., Wang, Y., Zbinden, R.M., 2014. Global distribution and trends of tropospheric ozone: an observation-based review. Elementa 2, 000029. http://dx.doi.org/10.12952/journal.elementa.000029.

Delany, A.C., Haagensen, P., Walters, S., Wartburg, A.F., Crutzen, P.J., 1985. Photochemically produced ozone in the emission from large-scale tropical vegetation fires. J. Geophys. Res. 90, 2425–2429.

Fenn, M.E., Bytnerowicz, A., Schilling, S.L., Ross, C.S., 2015. Atmospheric deposition of nitrogen, sulfur and base cations in jack pine stands in the Athabasca Oil Sands Region, Alberta, Canada. Environ. Pollut. 196, 497–510.

Fowler, C.T., 2003. Human health impacts of forest fires in the southern United States: a literature review. J. Ecol. Anthropol. 7, 39–63.

Goldammer, J.G., Statheropoulos, M., Andreae, M.O., 2009. Impacts of vegetation fire emissions on the environment, human health, and security: a global perspective. In: Bytnerowicz, A., Arbaugh, M., Riebau, A., Andersen, C. (Eds.), Wildland Fires and Air PollutionDevelopments in Environmental Science 8. Elsevier, Amsterdam, pp. 3–36.

Gregory, M., 2012. New life in a charred forest. Edmonton Journal, August 29, 2012.

Haikerwal, A., Akram, M., Del Monaco, A., Smith, K., Sim, M.R., Meyer, M., Tonkin, A.M., Abramson, M.J., Dennekamp, M., 2015. Impact of fire particulate matter ($PM_{2.5}$) exposure during wildfires on cardiovascular health outcomes. J. Am. Heart Assoc. 4, 1–10. http://dx.doi.org/10.1161/JAHA.114.001653.

Hanson, P.J., Lindberg, S.E., 1991. Dry deposition of reactive nitrogen compounds: a review of leaf, canopy and non-foliar measurements. Atmos. Environ. 25A, 1615–1634.

Hays, M.D., Geron, C.D., Linna, K.J., Smith, N.D., Schauer, J.J., 2002. Speciation of gas-phase and fine particle emissions from burning of foliar fuels. Environ. Sci. Technol. 36, 2281–2295.

Hegg, D.A., Radke, L.F., Hobbs, P.V., Riggan, P.J., 1988. Ammonia emissions from biomass burning. Geophys. Res. Lett. 15, 335–337.

Hsu, Y.-M., 2013. Trends in passively-measured ozone, nitrogen dioxide and sulfur dioxide concentrations in the Athabasca Oil Sands Region of Alberta, Canada. Aerosol Air Qual. Res. 13, 1448–1463.

Hsu, Y.-M., Bytnerowicz, A., 2015. Air pollution and dry deposition of nitrogen and sulphur in the AOSR estimated using passive samplers. In: Clair, T.A., Percy, K.E. (Eds.), Assessing Forest Health in the Athabasca Oil Sands Region. WBEA Technical Report, Fort McMurray, Alberta, Canada, 2015-05-25, pp. 8–39.

Hsu, Y.-M., Clair, T.A., 2015. Measurement of fine particulate matter water-soluble inorganic species and precursor gases in the Alberta Oil Sands Region using an improved semicontinuous monitor. J. Air Waste Manage. Assoc. 65, 423–435.

Hsu, Y.-M., Bytnerowicz, A., Fenn, M.E., Percy, K.E., 2016. Atmospheric dry deposition of sulphur and nitrogen in the Athabasca Oil Sands Region, Alberta, Canada. Sci. Total Environ. 568, 285–295.

Hyde, J.C., Blades, J., Hall, T., Ottmar, R.D., Smith, A., 2016. Smoke management photographic guide: a visual aid for communicating impacts. Gen. Tech. Rep. PNW-GTR-925. U.S. Department of Agriculture, Forest Service, Pacific Northwest Research Station, Portland, OR (59 pp.).

IPCC, 2013. Climate Change 2013: The Physical Science Basis. In: Stocker, T.F., Qin, D., Plattner, G.-K., Tignor, M., Allen, S.K., Boschung, J., Nauels, A., Xia, Y., Bex, V., Midgley, P.M. (Eds.), Working Group I Contribution to the Fifth Assessment Report of the Intergovernmental Panel on Climate Change. Cambridge University Press, Cambridge, United Kingdom and New York, NY, USA (27 pp.).

Jaffe, D., Wigder, N.L., 2012. Ozone production from wildfires; a critical review. Atmos. Environ. 51, 1–10.

Jaffe, D., Chand, D., Hafner, W., Westerling, A., Spracklen, D., 2008. Influence of fires on O_3 concentrations in the western U.S. Environ. Sci. Technol. 42, 5885–5891.

Johnston, K., Ver Hoef, J., Krivoruchko, K., Lucas, N., 2001. Using ArcGIS Geostatistical Analyst. ESRI, Redlands, California.

Kalberer, M., Ammann, M., Arens, F., Gaggeler, H.W., Baltensperger, U., 1999. Heterogenous formation of nitrous acid (HONO) on soot aerosol particles. J. Geophys. Res. 104, 13825–13832.
Kinney, P.L., 2008. Climate change, air quality, and human health. Am. J. Prev. Med. 35, 459–467.
Koelemeijer, R.B.A., Homan, C.D., Matthijsen, J., 2006. Comparison of spatial and temporal variations of aerosol optical thickness and particulate matter over Europe. Atmos. Environ. 40, 5304–5315.
Koutrakis, P., Sioutas, C., Ferguson, S.T., Wolfson, J.M., Mulik, J.D., Burton, R.M., 1993. Development and evaluation of a glass honeycomb denuder/filter pack system to collect atmospheric gases and particles. Environ. Sci. Technol. 27, 2497–2501.
Lammel, G., Cape, J.N., 1996. Nitrous acid and nitrite in the atmosphere. Chem. Soc. Rev. 25, 361–369.
LeBel, P.J., Cofer III, W.R., Levine, J.S., Vay, S.A., 1988. Nitric acid and ammonia emissions from a mid-latitude prescribed wetlands fire. Geophys. Res. Lett. 15, 792–795.
Lin, M., Horowitz, L.W., Oltmans, S.J., Fiore, A.M., Fan, S., 2014. Tropospheric ozone trends at Mauna Loa observatory tied to decadal climate variability. Nat. Geosci. http://dx.doi.org/10.1038/NGE02066.
Lin, M., Fiore, A.M., Horowitz, L.W., Langford, A.O., Oltmans, S.J., Tarasick, D., Rieder, H.E., 2015. Climate variability modulates western US ozone air quality in spring via deep stratospheric intrusions. Nat. Commun. 6, 7105. http://dx.doi.org/10.1038/ncomms8105.
Liu, Y., Goodrick, S., Heilman, W., 2014. Wildland fire emissions, carbon, and climate: wildfire-climate interactions. For. Ecol. Manag. 317, 80–96.
Lovett, G.M., 1994. Atmospheric deposition of nutrients and pollutants in North America: an ecological perspective. Ecol. Appl. 4, 629–650.
Oltmans, S.J., Lefohn, A.S., Shadwick, D., Harris, J.M., Scheel, H.E., Galbally, I., Tarasick, D.W., Johnson, B.J., Brunke, E.-G., Claude, H., Zeng, G., Nichol, S., Schmidlin, F., Davies, J., Cuevas, E., Redondas, A., Naoe, H., Nakano, T., Kawasato, T., 2013. Recent tropospheric ozone changes - a pattern dominated by slow or no growth. Atmos. Environ. 67, 331–351.
Percy, K.E., 2013. Ambient air quality and linkage to ecosystems in the Athabasca Oil Sands, Alberta. Geosci. Can. 40, 182–201.
Percy, K.E., Hansen, M.C., Dann, T., 2012. Air quality in the Athabasca Oil Sands Region 2011. In: Percy, K.E. (Ed.), Alberta Oil Sands: Energy, Industry and the Environment. Elsevier Press, Oxford, UK, pp. 47–91 http://dx.doi.org/10.1016/B978-0-08-097760-7.00004-4.
Pinder, R.W., Davidson, E.A., Goodale, C.L., Greaver, T.L., Herrick, J.D., Liu, L., 2012. Climate change impacts of US reactive nitrogen. PNAS 109, 7671–7675.
Pruchniewicz, P.G., 1973. The average tropospheric ozone content and its variation with season and latitude as a result of the global ozone circulation. Pure Appl. Geophys. 106-108, 1058–1073.
R Core Team, 2015. R: A Language and Environment for Statistical Computing. R Foundation for Statistical Computing, Vienna, Austria <https://www.R-project.org/>.
Rannick, Ü., Altimir, N., Mammarella, I., Bäck, J., Rinne, J., Ruuskanen, T.M., Hari, P., Vesala, T., Kulmala, M., 2012. Ozone deposition into a boreal forest over a decade of observations: evaluating deposition partitioning and driving variables. Atmos. Chem. Phys. 12, 12165–12182.
Roadman, M.J., Scudlark, J.R., Meisinger, J.J., Ullman, W.J., 2003. Validation of Ogawa passive samplers for the determination of gaseous ammonia concentrations in agricultural settings. Atmos. Environ. 37, 2317–2325.
Saarnio, K., Aurela, M., Timonen, H., Saarikoski, S., Teinila, K., Makela, T., Sofiev, M., Koskinen, J., Aalto, P.P., Kulmala, M., Kukkonen, J., Hillamo, R., 2010. Chemical composition of fine particles in fresh smoke plumes from boreal wild-land fires in Europe. Sci. Total Environ. 408, 2527–2542.
Schaap, M., van Loon, M., ten Brink, H.M., Dentener, F.J., Builtjes, P.J.H., 2004. Secondary inorganic aerosol simulations for Europe with special attention to nitrate. Atmos. Chem. Phys. 4, 857–874.
Schweizer, D., Cisneros, R., 2014. Wildland fire management and air quality in the southern Sierra Nevada: using the Lion Fire as a case study with a multi-year perspective on PM2.5 impacts and fire policy. J. Environ. Manag. 144, 265–278.
Seinfeld, J.H., Pandis, S.N., 2006. Atmospheric Chemistry and Physics. John Wiley & Sons, Inc., New York (1326 pp.).
Singh, H.B., Ludwig, F.L., Johnson, W.B., 1978. Tropospheric ozone - concentrations and variabilities in clean remote atmospheres. Atmos. Environ. 12, 2185–2196.
Stephens, S.L., Burrows, N., Buyantuyev, A., Gray, R.W., Keane, R.E., Kubian, R., Liu, S., Seijo, F., Shu, L., Tolhurst, K.G., van Wagtendonk, J.W., 2014. Temperate and boreal forest mega-fires: characteristics and challenges. Front. Ecol. Environ. 12, 115–122.
Tang, H.M., Lau, T., 2000. A new all season passive sampling system for monitoring ozone in air. Environ. Monit. Assess. 65, 129–137.
Tang, H.M., Brassard, B., Brassard, R., Peake, E., 1997. A new passive sampling system for monitoring SO_2 in the atmosphere. Field Anal. Chem. Technol. 1, 307–314.
Tang, H.M., Lau, T., Brassard, B., Cool, W., 1999. A new all-season passive sampling system for monitoring NO_2 in air. Field Anal. Chem. Technol. 3, 338–345.
The Royal Society, 2008. Ground-level ozone in the 21st century: future trends, impacts and policy implications. Science Policy, Report 15/08 (London).
Urbanski, S.P., Hao, W.M., Baker, S., 2009. Chemical Composition of Wildland Fire Emissions. In: Bytnerowicz, A., Arbaugh, M., Riebau, A., Andersen, C. (Eds.), Wildland fires and air pollutionDevelopments in Environmental Science 8. Elsevier, Amsterdam, pp. 79–107.
Wood Buffalo Environmental Association (WBEA), 2012. Wood Buffalo Environmental Association Annual Report 2011 (Fort McMurray, Alberta, Canada).
Zheng, M., Salmon, L.G., Schauer, J.J., Zeng, L., Kiang, C.S., Zhang, Y., Cass, G.R., 2005. Seasonal trends in PM2.5 source contributions in Beijing, China. Atmos. Environ. 39, 3967–3976.